



저작자표시-비영리-변경금지 2.0 대한민국

이용자는 아래의 조건을 따르는 경우에 한하여 자유롭게

- 이 저작물을 복제, 배포, 전송, 전시, 공연 및 방송할 수 있습니다.

다음과 같은 조건을 따라야 합니다:



저작자표시. 귀하는 원저작자를 표시하여야 합니다.



비영리. 귀하는 이 저작물을 영리 목적으로 이용할 수 없습니다.



변경금지. 귀하는 이 저작물을 개작, 변형 또는 가공할 수 없습니다.

- 귀하는, 이 저작물의 재이용이나 배포의 경우, 이 저작물에 적용된 이용허락조건을 명확하게 나타내어야 합니다.
- 저작권자로부터 별도의 허가를 받으면 이러한 조건들은 적용되지 않습니다.

저작권법에 따른 이용자의 권리는 위의 내용에 의하여 영향을 받지 않습니다.

이것은 [이용허락규약\(Legal Code\)](#)을 이해하기 쉽게 요약한 것입니다.

[Disclaimer](#)

The role of the prelimbic cortex-nucleus  
accumbens core circuit in the expression of  
cocaine sensitization and decision-making  
toward risk choice in a rat gambling task

Min Jeong Ku

Department of Medical Science  
The Graduate School, Yonsei University

The role of the prelimbic cortex-nucleus  
accumbens core circuit in the expression of  
cocaine sensitization and decision-making  
toward risk choice in a rat gambling task

Directed by Professor Jeong-Hoon Kim

The Doctoral Dissertation  
submitted to the Department of Medical Science,  
the Graduate School of Yonsei University  
in partial fulfillment of the requirements  
for the degree of Doctor of Philosophy

Min Jeong Ku

December 2022

This certifies that the Doctoral  
Dissertation of Min Jeong Ku is approved.

---

Thesis supervisor: Jeong-Hoon Kim

---

Thesis Committee Member#1: Jae-Jin Kim

---

Thesis Committee Member#2: Young-Chul Jung

---

Thesis Committee Member#3: Jung-Seok Choi

---

Thesis Committee Member#4: Yoonhee Jin

The Graduate School  
Yonsei University

December 2022

## ACKNOWLEDGEMENTS

2016년 2월 설렘과 기대감을 안고 연구실 생활을 시작하여 학위과정을 마무리하기까지 많은 과정을 되돌아보는 시간이 온 것에 감사합니다. ‘인간의 정신활동을 신경생물학적으로 어떻게 이해할 수 있을까?’라는 질문을 품고 시작했던 박사과정의 기간은 학문적으로 큰 배움을 얻은 시간이었을 뿐만 아니라 개인적으로도 한층 성장할 수 있는 시간이었습니다. 학문의 즐거움에도 불구하고 때로 힘들고 지치는 순간이 있었고, 그럴 때마다 인내하고 나아갈 수 있도록 도움과 격려를 주신 많은 분들께 이 지면을 빌려 감사의 인사를 드립니다.

먼저 이 모든 과정이 가능하도록 부족한 저에게 끊임없이 기회를 주시고 좋은 연구환경에서 마음껏 연구할 수 있도록 아낌없이 지원해주신 김정훈 지도교수님께 감사의 말씀을 드립니다. 교수님의 열정적이고 흥미진진한 강의와 이야기들을 통해 지적 호기심이 자극되었고, 연구에 대한 의지가 더욱 불타오르곤 했습니다. 또 특정한 연구결과가 어떻게 해석되며 어떤 의미를 가질 수 있는지, 연구결과들을 모아 어떻게 하나의 멋진 논문으로 탄생시키는지 배울 수 있었습니다. 때로 의욕이 앞서 중요한 것을 놓치곤 하던 저에게 바른 길을 알려주시고, 여러 사람과 함께 걷는 법을 알려주신 것은 앞으로도 오랫동안 인생의 자양분이 될 것입니다.

바쁘신 중에도 귀한 시간을 내어 연구계획 자문심사부터 본 심사에 이르기까지 부족한 점을 짚어 주시고 귀중한 조언을 해주신 김재진 교수님, 정영철 교수님, 최정석 교수님, 진윤희 교수님께도 감사

의 인사를 드립니다.

연구실에서 동고동락하며 서로 끌어주고 밀어주는 따스한 선후배님들에게도 감사의 인사를 전합니다. 어려움이 닥치면 가장 먼저 찾았던 김화영 연구교수님, 항상 발 벗고 나서서 문제를 해결해주시고 신선한 아이디어로 새로운 연구의 길을 열어주셔서 감사합니다. 저의 첫 사수로서 연구의 기초사항들을 꼼꼼히 알려주시고 따뜻하게 이끌어 주셨던 윤형신 연구교수님, 직접 제 손을 잡고 동물 핸들링과 주사 방법을 알려주셨던 것은 평생 잊지 못할 것 같습니다. 연구에 대한 열정을 따라잡을 수 없었던 채문정 박사님, 확신에 찬 격려가 정말로 큰 힘이 된 적이 많았습니다. 반대편에 있다가 어느새 교차점에서 만난 광명지 선배님, 함께 나누었던 수많은 대화 덕분에 연구와 사람에 대한 생각의 폭을 한층 넓힐 수 있었습니다. 오토 세팅부터 거의 모든 실험을 함께하며 같이 고생했고 반짝이는 아이디어로 문제를 해결해주었던, 이제는 전우애가 느껴지는 동료 박종우, 성실하게 본인의 실험을 이끌며 장비와 프로그램을 다루는 능력이 나날이 발전하고 있는 한준엽 후배님, 존재만으로도 큰 힘이 될 만큼 배려가 깊고 사랑스러운, 앞으로 더욱더 빛날 이서현 후배님, 누구보다 손이 빠르고 시간을 두 배로 활용하는 배울 점 많은 임하은 석사 후배님 모두 감사합니다. 졸업 후 각자의 자리에서 멋지게 자리 잡고 계신 조보람, 이정원 박사님, 그리고 연구 경험과 사회로 진출하신 경험을 바탕으로 유익한 이야기를 들려주시는 연구실 졸업생 선배님들 모두에게 감사 인사를 드립니다.

강의와 세미나를 통해 전공 지식을 불어넣어 주신 생리학 교실 교

수님들과 저의 연구에 관심을 가져주시고 응원해주신 생리학 교실 선생님들께도 이 기회를 통해 감사의 말씀을 전합니다. 힘들 때면 언제나 징징거릴 수 있었고 그럴 때마다 큰 힘을 주었던 저의 오랜 친구들에게도 감사 인사를 전하며, 멀리서나마 응원의 마음을 전해주셨던 친척분들께도 감사드립니다.

마지막으로 언제나 저의 결정을 지지해주시고 잘할 거라 믿어주시는 부모님과 묵묵하게 진심 어린 응원을 해주었던 언니, 동생에게 깊이 감사드립니다. 학위를 시작하며 멀리 떨어져 살게 되어 자주 만나지 못했지만, 가족이라는 울타리는 언제나 든든한 버팀목이었습니다. 베풀어주신 은혜와 응원에 좋은 모습으로 보답할 수 있도록 앞으로 더욱 노력하겠습니다. 사랑하고 감사합니다.

2022년 12월

구민정 드림

## <TABLE OF CONTENTS>

LIST OF FIGURES .....	iii
ABSTRACT .....	v
I. INTRODUCTION .....	4
II. MATERIALS AND METHODS .....	6
1. Animals .....	6
2. Drugs .....	6
3. Stereotaxic surgery .....	6
4. Cocaine-induced locomotor sensitization .....	7
A. Apparatus .....	7
B. Basal locomotor activity with optical stimulation .....	8
C. Cocaine sensitization with optical stimulation .....	8
5. The rat gambling task (rGT) .....	9
A. Apparatus .....	9
B. Pre-training .....	9
C. Gambling task .....	10
D. Optical stimulation during ITI .....	12
6. Tissue preparation and immunostaining .....	13

7. c-Fos imaging and cell-counting analysis, and histology .....	14
8. Golgi-Cox staining and dendritic spine imaging and analysis .....	14
9. Statistical analysis .....	15
III. RESULTS .....	17
1. The optogenetic stimulation of the PL-NAc core circuit has no effect on basal locomotor activity.....	17
2. The optogenetic stimulation of the PL-NAc core circuit inhibits cocaine-induced locomotor sensitization.....	19
3. The optogenetic stimulation of the PL-NAc circuit suppresses the cocaine-induced c-Fos expression in the NAc core.....	23
4. Optogenetic stimulation of the PL-NAc circuit inhibits the increase in mushroom spine density induced by repeated cocaine exposures .....	25
5. Optogenetic stimulation of the PL-NAc core circuits increases rats' preference toward risky choice in the risk-averse .....	28
6. The effects of the optical stimulation on behavioral parameters related with rGT appeared to vary according to risk preference .....	34
IV. DISCUSSION .....	38
V. CONCLUSION .....	44
REFERENCES .....	45
ABSTRACT (IN KOREAN) .....	56
PUBLICATION LIST .....	59

## LIST OF FIGURES

Figure 1. The optogenetic stimulation of the PL-NAc core circuit did not affect basal locomotor activity.....	18
Figure 2. The optogenetic stimulation of the PL-NAc core circuit inhibits cocaine-induced locomotor sensitization .....	21
Figure 3. The optogenetic stimulation of the PL-NAc core circuit reduced cocaine-induced c-Fos expression.....	24
Figure 4. Optogenetic stimulation of the PL-NAc core circuit suppressed the increase of mushroom spine density by cocaine .....	26
Figure 5. Optogenetic stimulation of the PL-NAc core circuit reduced the head diameter in thin spine .....	27
Figure 6. Schematic illustrations of optogenetic experimental procedures in rat gambling task .....	30
Figure 7. The risk-averse rats' preference for risky choice is increased by optical stimulation.....	32
Figure 8. The risk-averse rats' preference is shifted from the P2 to the P3 choice by 40 Hz optical stimulation .....	33

Figure 9. Comparison of behavioral parameters related with rGT between the recovery test and the opto-stimulation in the risk-averse rats .....	36
Figure 10. Comparison of behavioral parameters related with rGT between the recovery test and the opto-stimulation in the risk-seeking rats .....	37
Figure 11. An overview of the effects of optogenetic manipulation of the PL-NAc core circuit on cocaine sensitization and gambling-related behaviors in the rat gambling task (rGT) .....	43

## ABSTRACT

**The role of the prelimbic cortex-nucleus accumbens core circuit  
in the expression of cocaine sensitization  
and decision-making toward risk choice in a rat gambling task**

Min Jeong Ku

*Department of Medical Science*

*The Graduate School, Yonsei University*

(Directed by Professor Jeong-Hoon Kim)

Drug and behavioral addictions share clinical features, such as a craving and impulsive decision-making, and are highly comorbid. Common neural substrates may underlie their common characteristics and co-occurrence. The frontostriatal circuitry has been considered as the primary substrate mediating cravings and impaired decision-making. Animal models of addiction enable studying the role of a more specific circuit by allowing genetic or neuronal modulation. In this study, behavioral sensitization and the rat gambling task were used as representative animal models of drug and gambling addictions. Behavioral sensitization has been used to investigate the neural mechanism

underlying drug craving and can be strongly induced by psychomotor stimulants such as cocaine and amphetamine. The rat gambling task (rGT), a rat version of the Iowa gambling task, enables assessing rats' impulsive decision-making and exploring underlying neural mechanisms. Although it has been reported that some brain regions including the prelimbic cortex (PL) and the nucleus accumbens core (NAc core) are implicated in both cocaine craving and impulsive decision-making, the role of the neural circuit between the PL-NAc core remains unclear. Therefore, this study was designed to examine whether the PL-NAc core contributed to the modulation of cocaine-induced behavioral sensitization and impulsive decision-making in the rGT. Wireless optogenetics was adopted to selectively manipulate the specific neural circuit and minimize restriction of animals' movements. In the cocaine sensitization experiment, optogenetic stimulation of the PL-NAc core significantly inhibited cocaine-induced locomotor sensitization on day 7 compared to day 1. This effect was accompanied by attenuation of the increase in c-Fos expression and mushroom spine density in the NAc core. These results indicate that altered PL-NAc core activity could contribute to weakening cocaine craving through altering mushroom spine density. In the rGT experiment, optogenetic stimulation of the PL-NAc core immediately prior to decision-making differentially influenced impulsive choice according to risk preference. The risk-averse rats showed increased impulsive choices with optogenetic stimulation, which resulted from the decreased P2 and increased P3 choices. However, the risk-seeking rats did not change their choice preference with the same optogenetic stimulation, but they showed increased reward collection latency and food-tray entries. These results imply that the PL-NAc core activity

prior to decision-making may differ according to the risk preference, and the different neural activities may differentially contribute to impulsive decision-making or motivation for gambling behavior. Taken together, the findings of this study suggest that the PL-NAc core circuit may contribute to the modulation of cocaine craving and differentially mediate impulsive decision-making or motivation for gambling according to the risk preference.

---

Key words : prelimbic cortex, nucleus accumbens core, cocaine sensitization, rat gambling task, wireless optogenetics

**The role of the prelimbic cortex-nucleus accumbens core circuit  
in the expression of cocaine sensitization  
and decision-making toward risk choice in a rat gambling task**

Min Jeong Ku

*Department of Medical Science*

*The Graduate School, Yonsei University*

(Directed by Professor Jeong-Hoon Kim)

## **I. INTRODUCTION**

Drug addiction is a neuropsychiatric disorder characterized by intense drug craving, loss of control in limiting drug intake, and compulsive use of drugs despite negative consequences.<sup>1,2</sup> Behavioral addictions such as gambling and internet gaming disorders share core clinical features with drug addictions, which include cravings and impaired decision-making.<sup>3,4</sup> In addition, behavioral addictions are highly comorbid with drug addiction, and this comorbidity is often accompanied with increased severities of addiction and psychopathological symptoms.<sup>5-8</sup>

These overlapped clinical features and co-occurrence may be caused by common neural substrates mediating drug and behavioral addictions. Central to drug addiction is the brain reward pathway, in which addictive drugs can cause structural, physiological, and functional changes. The brain reward pathway is an interconnected neural circuitry that comprises the prefrontal cortex (PFC), dorsal and ventral striatum,

ventral tegmental area, and amygdala.<sup>9,10</sup> Among them, the nucleus accumbens (NAc), a major component of the ventral striatum, plays an essential role in reward processing, craving, aversion, and reinforcement learning by integrating signals from the limbic and cortical areas.<sup>1,11,12</sup> The NAc receives glutamatergic inputs from the PFC, amygdala, and hippocampus.<sup>13</sup> Among these regions, the PFC plays a central role in reward anticipation, control of craving and inhibition, and decision-making.<sup>14</sup> Dysfunction of the frontostriatal circuitry including the PFC-NAc may contribute to the development of cravings and impaired decision-making in patients with drug addiction.<sup>14,15</sup> For example, the frontostriatal activities were found to correlate with the self-report craving level in cocaine-dependent individuals.<sup>16,17</sup> In addition, methamphetamine users showed stronger activation in the ventral striatum but weaker activation in the right dorsolateral PFC during a risky decision-making task.<sup>18</sup>

Recently, a growing number of functional neuroimaging studies have reported that the frontostriatal circuitry is also implicated in behavioral addiction.<sup>19,20</sup> For example, abnormal functional connectivity in the frontostriatal circuitry is associated with the magnitude of cravings in gambling and internet gaming disorders as well as substance use disorders including cocaine, alcohol, and nicotine addictions.<sup>21-26</sup> In addition, altered frontostriatal activities are involved in impaired decision-making, which involves making a choice that brings an immediate reward effect of the drug even at the risk of incurring future negative outcomes.<sup>27,28</sup> Patients with gambling, internet gaming, or substance use disorders demonstrate a preference for immediate rewards, which is an impulsive choice, and show the altered frontostriatal activities during the decision-making process compared with healthy controls.<sup>18,29-34</sup>

Although numerous clinical studies have revealed that the frontostriatal circuitry is commonly involved in the cravings and impaired decision-making in drug and behavioral addictions, the role of a more specific pathway within the frontostriatal circuitry requires further investigation to improve treatment strategies for comorbid

drug and behavioral addictions. In this sense, animal models of addiction can play an essential role in translational studies by allowing genetic or neuronal modulation while controlling for environmental factors.<sup>35</sup>

One of the widely used animal models of drug addiction is behavioral sensitization, which is used to investigate the neural mechanisms underlying the intensification of drug cravings observed in human addicts. Behavioral sensitization refers to the progressive augmentation of behavioral responses by repeated drug administration, and it is strongly induced by psychomotor stimulants, such as cocaine and amphetamine. This effect persists even after long periods of drug-free withdrawal.<sup>36,37</sup> Behavioral sensitization involves structural and functional alterations in the medial PFC (mPFC) and the NAc.<sup>38,39</sup> Administration of cocaine or amphetamine activates neurons in the mPFC and NAc, which can be measured by increased mRNA or protein expression of the immediate early genes, such as c-Fos.<sup>40-42</sup> Further, both cocaine and amphetamine induce robust increases in the dendritic spine density in the NAc, and the increased spine density is maintained after drug withdrawal periods, suggesting its role in the incubation of drug craving.<sup>43-45</sup>

In rodents, the mPFC is subdivided into the prelimbic (PL) and infralimbic (IL) cortices, with the PL neurons primarily projecting to the NAc core and the IL neurons to the NAc shell.<sup>46,47</sup> The distinct roles of those two subdivisions of the mPFC or the mPFC-NAc circuit in behavioral sensitization have been reported. For example, the excitability of the PL neurons was significantly increased, whereas that of the IL neurons was reduced during the extinction after cocaine self-administration.<sup>48</sup> Increased c-Fos expression in the PL neurons specifically innervating the NAc core was proportional to cocaine-seeking behavior, but this was not the case in the IL innervating the NAc shell.<sup>49</sup> Chemogenetic inhibition of the PL-NAc core circuit suppressed cue-induced cocaine relapse, whereas chemogenetic activation of the IL-NAc shell circuit reduced it.<sup>50,51</sup> These findings suggest the importance of

circuit-specific studies in addiction-related behaviors.

The rat gambling task (rGT) is a distinct and unique animal model of gambling disorder, which allows us to investigate the neural mechanisms underlying gambling-related decision-making.<sup>52-54</sup> The rGT was developed based on fundamental principles of the Iowa gambling task (IGT), which is widely adopted to assess human decision-making in the study of gambling behavior.<sup>55,56</sup> With the IGT, participants play a gambling game and make a series of card choices from four decks, where each choice can lead to winning or losing varying amounts of hypothetical money. Two decks yield immediate large rewards but long-term losses because of the increased chance of penalties; thus, these are risky options and indicative of an impulsive choice. The other two decks yield immediate small rewards but long-term gains because of the low chance of penalties; thus, these are advantageous.<sup>57,58</sup> While healthy participants develop a preference for the advantageous decks, patients with prefrontal damage, drug addiction, gambling or internet gaming disorders, show a preference for the disadvantageous options.<sup>29,59-62</sup>

Like the IGT, the rGT assigns four options with different reward amounts, punishment time, and reward/punishment probabilities, which enables assessment of rats' impulsive choices. Similar to the human studies with the IGT, addictive drugs can alter rats' impulsive choices in rGT. For example, rats repeatedly exposed to cocaine showed increased preferences for impulsive choices.<sup>56,63</sup> Furthermore, it has been shown that the neuronal activities in the PL and NAc core were positively correlated with impulsive choices.<sup>64,65</sup> Conversely, impulsive choices were increased by excitotoxic lesions of the NAc core or pharmacological inactivation of the PL.<sup>66,67</sup> Since such conflicting results could be due to nonspecific manipulations or detection of neuronal activities, a more precisely controlled study is required.

Optogenetics allows cell-type or pathway-specific manipulation of brain circuitry using cell-type-specific promoters or a recombinase-dependent virus or via

illumination of axonal projections. Moreover, this technique enables manipulation of the neural activity at millisecond timescales. Thus, optogenetics is well-suited to study neural mechanisms underlying complex cognitive process including cravings and decision-making.<sup>68</sup> A few studies have shown that optogenetic manipulation of the mPFC-NAc circuit or the NAc region could regulate drug craving and risky decision-making. For example, it has been reported that cocaine-induced behavioral sensitization was abolished by optogenetic stimulation of the IL-NAc shell circuit, and risky choice could be regulated by optogenetic stimulation of the NAc neurons.<sup>69,70</sup> However, it has not been studied yet, to my knowledge, how the optogenetic manipulation of PL-NAc core regulates behavioral sensitization and impulsive decision-making.

To address these issues, the present study is aimed at investigating the roles of the PL-NAc core circuit in animal models of drug and behavioral addictions. Behavioral sensitization and the rGT were used as representative animal models of psychostimulant use or gambling disorders, and these animal models could assess drug craving and impulsive choice, respectively. Optogenetic techniques were used to selectively manipulate the PL-NAc core circuit during behavioral experiments. In particular, recently developed wireless techniques combined with optogenetics were adopted to minimize human intervention and restriction of animals' movement during behavioral experiments.<sup>71,72</sup> Based on previous findings, I hypothesized that optogenetic manipulation of the PL-NAc core would influence the expression of cocaine-induced locomotor sensitization by modulating the neuronal activity and the dendritic spine density in the NAc core, and further it may alter impulsive decision-making in the rGT.

## II. MATERIALS AND METHODS

### 1. Animals

Male Sprague-Dawley rats (9 weeks old for the cocaine sensitization, 3 weeks old for the rGT) were obtained from Orient Bio Inc. (Seongnam-si, Korea). They were housed as two per cage in a 12-h light/dark cycle room (lights out at 8:00 pm) and all experiments were conducted during the daytime.

The rats for sensitization had access to food and water *ad libitum*, whereas the rats for rGT received restricted diet that lowered their body weight to 85 % of normal levels to increase their motivation to the rGT. The restricted diet started 2 days before the pre-training experiments and were maintained until the end of experimentation. All experiments were started a week after arrival to allow habituation to a new colony environment. All animal use procedures were conducted according to an approved Institutional Animal Care and Use Committee protocol of Yonsei University College of Medicine.

### 2. Drugs

Cocaine hydrochloride was purchased from Belgopia (Louvain-La-Neuve, Belgium). It was dissolved in sterile 0.9% saline to a final concentration of 15 mg/ml.

### 3. Stereotaxic surgery

Rats were anesthetized with intraperitoneal (IP) ketamine (100 mg/kg) and xylazine (6 mg/kg), placed on a stereotaxic instrument with the incisor bar at 5.0 mm above the interaural line. After skull surface were exposed, a pair of bilateral infusion cannulas (28 gauge; Plastics One, Roanoke, VA) connected to 1  $\mu$ l syringes (Hamilton, Reno, NV) via PE-20 tubing was angled at 10° to the vertical and aimed at the NAc core

(A/P, +3.2; L,  $\pm 2.8$ ; D/V,  $-7.1$  mm from the bregma and skull),<sup>73</sup> delivering retrograde AAV expressing Cre recombinase (AAVrg-hSyn-Cre, viral titer  $7 \times 10^{12}$  vg/ml) (Addgene, Watertown, MA; the Addgene plasmid #105553 used to prepare this virus was a gift from Dr. James M. Wilson) and at the PL (A/P +3.2, L  $\pm 1.3$ , D/V  $-4.1$  mm from the bregma and skull),<sup>51</sup> delivering Cre-dependent AAV expressing ChR2-EYFP or EYFP alone (AAV5-EF1 $\alpha$ -DIO-hCHR2-(H134R)-EYFP or AAV5-EF1 $\alpha$ -DIO-EYFP, viral titer  $1 \times 10^{13}$  vg/ml) (Addgene, Watertown, MA; the Addgene plasmids #20298 and #27056 used to prepare these viruses were gifts from Dr. Karl Deisseroth). Then, the syringes were placed on an infusion pump (KD Scientific, Holliston, MA) and the 0.5  $\mu$ l of AAV was infused at a rate of 0.1  $\mu$ l/min for 5 min with an additional 5 min allowed for its diffusion.

For implantation of the opto-device, the incisor bar was lowered to 0.0 mm. The bilateral microscale inorganic light-emitting diodes ( $\mu$ -ILED) probes were vertically inserted aiming at the far posterior site of the NAc right below the bregma (A/P +0.5, L  $\pm 2.0$ , D/V  $-7.5$  mm from the bregma and skull),<sup>51</sup> and the device was secured with dental acrylic cement anchored to stainless steel screws fixed to the skull. The rats were returned to their home cages for 2~3 weeks of recovery and viral expression period.

## **4. Cocaine-induced locomotor sensitization**

### **A. Apparatus**

Locomotor activity was measured with a bank of nine activity boxes ( $35 \times 25 \times 40$  cm<sup>3</sup>) (IWOO Scientific Corporation, Seoul, Korea) made of translucent Plexiglas. Each box was individually housed in a polyvinyl chloride plastic sound-attenuating cubicle. The floor of each box consisted of 21 stainless steel rods (5 mm diameter) spaced 1.2 cm apart center-to-center. Two infrared light photobeams (Med Associates,

St. Albans, VT), positioned 4.5 cm above the floor and spaced evenly along the longitudinal axis of the box, estimated locomotor activity. Locomotor activity was counted only when two beams were consecutively interrupted. In this way, any confounding measures like grooming in a spot covering just a single beam was avoided from the counts.

### **B. Basal locomotor activity with optical stimulation**

Three weeks after the surgery, on day 0, the rats were randomly assigned to two groups: 40 Hz optical stimulation and no stimulation, to assess the effect of optical stimulation on the basal locomotor activity. In a sub-group of optical stimulation, a wireless module with a rechargeable battery was connected into the opto-device mounted on the rat skull and a protective cap was placed to cover the module. The set of the opto-device, the module, and the battery was paired with a smartphone through Bluetooth and operated using a customized smartphone app. Optical stimulation was delivered as repeated blue lights (470 nm) for 5 min (40 Hz, 30 s on/off) with an interval of a light-free period for 10 min throughout the 60 min locomotor activity measurement. The number of rats used in the experiment were as follows: no stimulation (22), 40 Hz optical stimulation (23).

### **C. Cocaine sensitization with optical stimulation**

On the next day, the rats were re-assigned to three groups evenly from two groups on day 0: saline, cocaine only, and cocaine with optical stimulation. They were administered with saline or cocaine (15 mg/kg, i.p.) once per day for 7 consecutive days, and their locomotor activities were measured on days 1 and 7. No activities were measured during home-cage injections for the rest of days. The rats were first habituated to the activity boxes for 30 min, and their locomotor activities were

measured for 60 min immediately following saline or cocaine injections. This procedure is well known to produce enduring sensitization of the locomotor response to cocaine.<sup>74,75</sup> While measuring locomotor activities on days 1 and 7, only a sub-group of cocaine with optical stimulation received repeated blue lights as described above. The number of rats used in the experiment were as follows: saline (15), cocaine only (14), and cocaine with optical stimulation (16).

## **5. The rat gambling task (rGT)**

### **A. Apparatus for the rGT**

The rGT was conducted in a set of eight identical touchscreen-based automated operant chambers housed in dense sound- and light-attenuating boxes (68.6 cm high × 60.7 cm long × 53.5 cm wide) (Campden Instruments Ltd., Leics, UK). Each chamber is equipped with a house light (light-emitting diode), touch-sensitive liquid crystal display monitor (touchscreen; 15.0 inch, screen resolution 1,024×768), pellet dispenser, and food magazine unit (with light and infrared beam to detect entries) facing the touchscreen. Whisker Standard Software (Campden Instruments, Ltd., Leics, UK) was used as the controlling software, and two computers were used to control the four chambers each.

### **B. Pre-training**

Rats were trained once daily in a 30 min session, 5 days per week. Sucrose pellets (45 mg) (Bio-Serve, Flemington, NJ, USA) were used as a reward. In stage 1, the rats were first habituated to the touchscreen chamber for one session. In stages 2 and 3, which lasted over 4 to 5 daily sessions, rats were trained to learn the relationship between the light stimulus on the screen and the reward pellet, and to touch the screen to receive a pellet as a reward. In this stage, the inter trial interval

(ITI) of the 5 sec rule was first applied such that rats have to wait for 5 sec after pushing their noses into the food magazine to start a new trial. In stage 4, which lasted over 13 to 15 daily sessions, the rats serially learned to touch one of the four windows which are randomly lit, within different stimulus durations (starting from 40 sec, then serially reduced to 20, and finally, 10 sec), to receive one pellet. Sessions were completed within 100 trials or 30 min, whichever comes first. In this stage, the rats learn for the first time that they are punished with a time-out (i.e., the white house-light is lit for 5 sec) if they touch the screen without waiting during ITI (premature response) or if they do not touch the screen within the stimulus duration (omission). They were also punished if they touched other windows which are not lit (incorrect). When the accuracy was greater than 80% and omissions was lower than 20%, the rats were considered to have acquired the task successfully.

### **C. Gambling task**

Essentially, during rat gambling task, rats were confronted with four choices differing in their probability and magnitude of reward (food) and punishment (time-out), and they had to learn an optimal strategy to determine the choice that provided the most reward per session. In stage 5 (rGT forced choice), which lasted over 7 daily sessions, rats learned for the first time the relationship between each window and the reward/punishment ratio assigned to that window. Touch on the first window (P1) produced 1 pellet (90%) or 5 sec time-out (10%); the second window (P2), 2 pellets (80%) or 10 sec time-out (20%); the third window (P3), 3 pellets (50%) or 30 sec time-out (50%); and the fourth window (P4), 4 pellets (40%) or 40 sec time-out (60%). In this stage, one of the four windows was randomly lit for 10-sec and rats are punished (i.e., the white house light is lit for 5 sec) for a premature response. Additionally, for the first time in this stage, rats were punished (time-out; i.e., the white house light is lit, and the window on the screen simultaneously flash for 5 to 40

sec) even on correctly touching the screen according to the pre-designated schedule for each window.

Unlike stage 5, four windows were simultaneously lit and rats were allowed to freely choose one of the four windows in stage 6 (rGT free choice). The reward and punishment settings designated for each window were the same as those introduced in stage 5, as well as ITI and stimulus duration time. Depending on which window rats chose, they received either reward (pellet) or punishment (time-out) with differently programmed probabilities. Once a trial was finished, regardless of the outcome, they again encountered four different choices in the next trial, and this process was repeated for 30 min. Hypothetically, if one window is chosen exclusively, the amount of reward pellets per session that an animal can obtain will be as follows: P1, 295; P2, 411; P3, 135; and P4, 99 pellets. The percentage of choices ( $[\text{number of choices for a specific window} / \text{total number of choices made}] \times 100$ ) was used to measure the rats' preferences for the different windows. After 20 daily sessions were completed, the average of the last three daily sessions' choice percentages was considered as a basal score for the rats' risk-preference. Rats were categorized as risk-averse when their basal score for P2 (the best optimal choice) was equal to or higher than 60%, whereas they were categorized as risk-seeking when it was lower than 60%. To avoid any location bias, windows were allocated in a counterbalanced way as follows: for half of the rats, the windows were 1 (P1), 2 (P4), 3 (P2), and 4 (P3); for the other half of the rats, the windows were 1 (P4), 2 (P1), 3 (P3), and 4 (P2).

Choice-related behavioral parameters were also measured during the rGT sessions. The percentage of premature response, which indicates impulsive action, was calculated as  $[\text{premature response} / \text{total initiated trials (omission + premature + choice response)}] \times 100$ . Omission percentage, which indicates attention or motivation to the task, was calculated as  $[\text{omission} / (\text{omission} + \text{choice response})] \times 100$ . Perseverative response ratio, which measures repeated screen touch during

punishment, was calculated as (total number of screen touches during punishment / the total number of punishment trials). Food-tray entries during ITI per trial, which measures repeated entry of the food magazine during ITI, was calculated as [the number of feed-tray entries during ITI / total initiated trials (omission + premature + choice response)]. Food-tray entries during stimulus duration per trial was calculated as [the number of feed-tray entries during stimulus duration / choice response]. Food-tray entry entries during loss timeout per 5 sec was calculated as [the number of feed-tray entries during ITI / total loss timeout time  $\times$  5]. Reward collection latency (the time required for rats to enter the food magazine to obtain the reward after a screen touch when it was rewarded) and choice response latency (the time required for rats to touch one of the four illuminated screens, after the end of the ITI) were also analyzed.

#### **D. Optical stimulation during ITI**

For the automated operation of the opto-device during every inter-trial interval (ITI), a photodetector-based wireless closed-loop optogenetic system was utilized. Photodetectors were attached for detecting screen, house, and food-magazine lights, and electric wires from the photodetectors were connected to a Bluetooth Low Energy Microcontroller unit (BLE MCU) board (Nordic Semiconductor, Trondheim, Norway). 20 Hz or 40 Hz optical stimulation was programmed to be delivered only when all lights were detected to turn off during the ITI. When any light was detected to turn on, the BLE MCU board sent a LED-off signal. During the opto-rGT, the opto-device mounted on the rat skull was connected with the wireless module with the rechargeable battery and the protective cap was placed to cover the module. The set of the opto-device, the module, and the battery was wirelessly paired with the BLE MCU board and operated automatically during every ITI. The intact wireless and selective operation of multiple opto-devices was validated before each session begins. The

numbers of rats for each group were as follows: averse-EYFP (9), averse-ChR2 (11), seeking-EYFP (17), seeking-ChR2 (32).

## **6. Tissue preparation and immunostaining**

In the cocaine sensitization experiment, perfusion was conducted 30 min and 90 min after saline or cocaine injection on day 7 to analyze dendritic spine morphology and c-Fos expression in the NAc core, respectively. In the rGT experiment, perfusion was carried out on the next day after the rGT.

The rats were deeply anesthetized with ketamine (100 mg/kg) and xylazine (6 mg/kg) and then perfused transcardially with 10 mM PBS (pH 7.4) followed by 4 % paraformaldehyde solution. Brains were removed and post-fixed in ice-cold 4 % paraformaldehyde solution for 24 hrs, followed by cryoprotection in 30 % sucrose solution at 4 °C for 3 days, and stored at -80 °C. Free-floating coronal sections (50  $\mu$ m) from frozen tissue blocks were prepared on a freezing microtome (HM 525, Fisher Scientific, Waltham, MA, USA). Sections were blocked for 1 hr in 10 mM PBS containing 5 % normal goat serum (Jackson ImmunoResearch Laboratories, West Grove, PA, USA) and 0.3 % triton X-100. Then they were incubated overnight at 4 °C with anti-c-Fos (1:2000) (Cell Signaling, Beverly, MA, USA) and anti-NeuN antibodies (Abcam, Cambridge, UK) diluted in 10 mM PBS containing 2 % normal goat serum and 0.1 % triton X-100. Following overnight incubation, the sections were rinsed with 0.1 % triton X-100 three times, and then they were incubated with anti-rabbit secondary antibodies conjugated with Alexa 405 and 594 (1:2000; Invitrogen, Waltham, MA, USA) for 2 hrs at room temperature. After rinsed with 0.1 % triton X-100 three times, the sections were transferred on slide glasses and then mounted with Vectashield mounting medium (H1400; Vector Laboratories, Peterborough, UK).

## **7. c-Fos imaging and cell-counting analysis, and histology**

About 10 images co-labelled with c-Fos and NeuN were acquired each from the PL and the NAc core. The images that had inappropriate signals or damaged regions were excluded from the final data. All images were acquired under the LSM710 confocal laser scanning microscope (Carl Zeiss, Oberkochen, Germany) with a 405 nm laser diode for NeuN, a 488 nm argon laser for EYFP, and a 594 nm HeNe laser for c-Fos. The thickness of the images was 6  $\mu\text{m}$  and obtained using 20x objective (numerical aperture 0.8) with 0.6x digital zoom. All images were taken with a resolution of 1024 pixels in x-y dimensions.

Cell-counting was performed using Zen desk software (Carl Zeiss) which semi-automatically counted the number of NeuN cells and a portion of them including c-Fos expression. Minimum areas of the cells containing c-Fos or NeuN signals were optimized according to the size of the cells or signals in the PL and NAc core, and fixed during all analysis. Smooth and Sharpen settings were also optimized and fixed. Exceptionally, a threshold of each image was manually set up depending on the quality of the image by two experimenters blind to the experimental groups. The level of EYFP or ChR2-EYFP expression was also manually assessed. The final data were obtained by averaging the two experimenters' results. The numbers of rats used for each group were as follows: saline (7), cocaine only (7), and cocaine with optical stimulation (8). Six images were used per rat.

## **8. Golgi-Cox staining and dendritic spine imaging and analysis**

The Golgi-Cox staining method previously reported was used.<sup>76</sup> In brief, brain tissues were immersed in the Golgi-Cox solution for 2 days in darkness at room temperature. The tissues were transferred into the fresh Golgi-Cox solution and incubated for 14 days. The tissues were stored in 30 % sucrose solution for 3 days in

4 °C. Coronal sections (100 μm) from the tissues were prepared on a freezing microtome (Fisher Scientific) and mounted onto the slide glasses with Permount mounting medium (Fisher Scientific).

For the analysis of dendritic spine morphology, confocal reflection mode was used.<sup>77</sup> One to three dendrites per neuron and 10 to 15 neurons per sample were acquired using the LSM710 confocal laser scanning microscope (Carl Zeiss) with a 488 nm argon laser and reflection mode (MBS T80/R20). z-stack images spaced with 0.349 μm were obtained using 63x oil-immersion objective (numerical aperture 1.4) and 3.0x digital zoom. All images were taken with a resolution of 1024 pixels in the x dimension, and the y dimension within the frame was cropped to ~300 μm depending on the dendritic shape. The final voxel size was  $0.044 \times 0.044 \times 0.349 \mu\text{m}^3$  in x-y-z plane. The analysis of spines was performed using NeuronStudio software which semi-automatically counts and classifies spines into three types (thin, mushroom, stubby) according to the classification dimensions (i.e., head to neck ratio, minimum height).<sup>78</sup> The minimum and maximum spine height values were set at 0.5 μm and 3.0 μm, respectively. Minimum stubby size was 15 voxels. The miss-counted spines were manually edited by two experimenters who were blind to the sample group, and the final data was obtained by averaging the two results. The average head diameter and length, as well as the density of each spine subtype, were calculated from each image. The numbers of rats and neurons for each group were as follows: saline (5 rats), cocaine only (4 rats), and cocaine with optical stimulation (5 rats). 10 to 15 neurons were used per rat.

## 9. Statistical analysis

Data were shown as mean + standard error of the mean (SEM), and all data were analyzed using SigmaPlot (version 12.0) and graphed using Graphpad Prism (version

7.0) software. T-test was used to compare the mean of two groups. One-way analysis of variance (ANOVA) was used to compare the ratio of c-Fos+ neurons and the density, head diameter, and length of dendritic spines. Two-way repeated measures ANOVA was used when there were two factors (virus  $\times$  optical stimulation, group  $\times$  time, and virus  $\times$  time) as between-within factors. ANOVAs were followed by *post hoc* Tukey or Bonferroni t-test. Differences between experimental conditions were considered statistically significant when  $p < 0.05$ .

### III. RESULTS

#### 1. The optogenetic stimulation of the PL-NAc core circuit has no effect on basal locomotor activity

To selectively manipulate the activity of the PL-NAc circuit by light, a viral set for Cre-dependent channelrhodopsin-2 (ChR2) expression and the wireless head-mounted opto-device were used. ChR2-EYFP was specifically expressed in the PL-NAc core circuit by injecting the retrograde adeno-associated virus (AAV) expressing Cre recombinase into the NAc core and the AAV expressing Cre-dependent ChR2 into the PL. Simultaneously, the opto-device was implanted on the rat skull, inserting bilateral probes with  $\mu$ -ILED at the far posterior site of the NAc (Figure 1A). Schematic diagram of the opto-device (Figure 1B) and a rat image with this device attached (Figure 1C) are shown.

Three weeks after the surgery of viral infusion and the opto-device implantation, the PL-NAc core circuit was stimulated by light to examine whether it affects basal locomotor activity. The wireless module with the rechargeable battery was connected into the opto-device mounted on the rat skull, which was controlled by the customized smartphone app. Optical stimulation was delivered as repeated blue lights (470 nm) for 5 min (40 Hz with 10 ms pulse width, 30 s on/off) (Figure 1D) with an interval of a light-free period for 10 min throughout the 60 min locomotor activity measurement. It was revealed that the optogenetic stimulation of the PL-NAc core circuit did not affect basal locomotor activity. Locomotor activity counts for 60 min were not different between groups ( $t_{43} = 0.198$ ,  $p = 0.844$ ) (Figure 1E). Two-way ANOVA conducted on time-course data shown as locomotor activity counts at 5 min intervals also revealed no differences in the effects of group [ $F_{1,43} = 0.485$ ,  $p > 0.05$ ] and group  $\times$  time interaction [ $F_{11,473} = 1.669$ ,  $p > 0.05$ ] (Figure 1F).

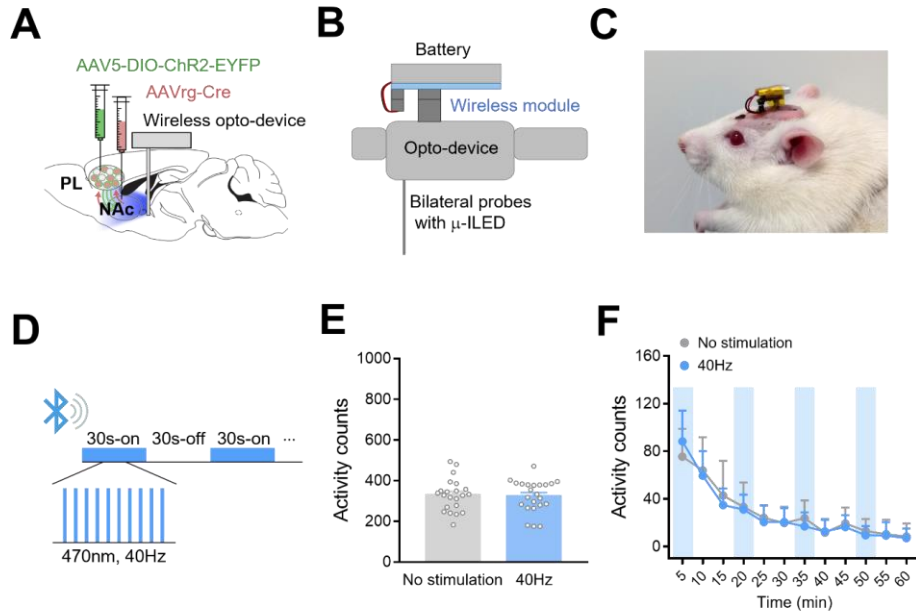


**Figure 1. The optogenetic stimulation of the PL-NAc core circuit did not affect basal locomotor activity.** (A) Schematic illustration of viral infusion and  $\mu$ -ILED probe insertion. Retrograde AAV-Cre virus was injected into the NAc core and Cre-dependent AAV5-ChR2-EYFP into the PL. Bilateral probes of the opto-device were inserted at the far posterior site of the NAc. (B) Schematic diagram of the opto-device connected with a wireless module and rechargeable battery. (C) A photo image for a rat taken after surgery of the viral infusion and the opto-device implantation. (D) Optical stimulation was delivered as repeated blue lights (470 nm) for 5 min (40 Hz with 10-ms pulse width, 30 s on/off) with an interval of a light-free period for 10 min throughout the 60 min locomotor activity measurement. (E) Locomotor activity counts for a total of the 60 min test were not changed by 40 Hz optical stimulation. (F) Time-course data shown as locomotor activity counts at 5 min intervals during the 60 min test. The light blue bar indicates optical stimulation delivered (5, 20, 35, and 50 min). Data are shown as mean + SEM. The number of rats for no stimulation group was 22, and 40 Hz optical stimulation was 23.

## **2. The optogenetic stimulation of the PL-NAc core circuit inhibits cocaine-induced locomotor sensitization**

Next, the effects of optogenetic stimulation of PL-NAc core on behavioral sensitization was examined by adopting a well-known cocaine-induced locomotor sensitization scheme.<sup>74,75</sup> The day after basal locomotor activity test, the rats were randomly assigned to three groups: saline, cocaine only, and cocaine with optical stimulation. They were administered with either saline or cocaine (15 mg/kg, i.p.) once per day for 7 consecutive days, and their locomotor activities were measured on days 1 and 7. The rats were first habituated to the activity boxes for 30 min, and their locomotor activities were measured for 60 min immediately following saline or cocaine injections. While measuring locomotor activities on days 1 and 7, only one group (cocaine with optical stimulation) received repeated blue light stimulation (Figure 2A).

As expected, rats exposed to daily cocaine showed a more profound sensitized locomotor response on day 7 compared with day 1 ( $p < 0.001$ ). This effect, however, was significantly inhibited by concurrent optical stimulation. The two-way ANOVA indicated that there are multiple significant effects on locomotor activity of groups [ $F_{2,42} = 25.137$ ,  $p < 0.001$ ], days [ $F_{1,42} = 6.015$ ,  $p < 0.05$ ], and interactions between groups and days [ $F_{2,42} = 14.307$ ,  $p < 0.001$ ]. Post-hoc Bonferroni t-test revealed that optical stimulation significantly decreased ( $p = 0.001$ ) the sensitized locomotor activity produced by cocaine on day 7 (Figure 2B). In time-course data shown as locomotor activity counts at 5 min intervals on day 7, the sensitized locomotor activity persisted for an entire hour of testing, whereas the optical stimulation apparently inhibited this effect. The two-way ANOVA revealed significant effects on locomotor activity of groups [ $F_{2,42} = 36.039$ ,  $p < 0.001$ ] and interactions between groups and times [ $F_{22,462} = 5.006$ ,  $p < 0.001$ ]. Post-hoc Bonferroni t-test revealed that the sensitized locomotor activity was significantly decreased by optical stimulation at 5

through 40, and 50 min time points, compared with that of cocaine only group (Figure 2C). After the experiments, robust expression of ChR2-EYFP in both PL and NAc core regions and accurate location of probe implantation were confirmed (Figure 2D, E).

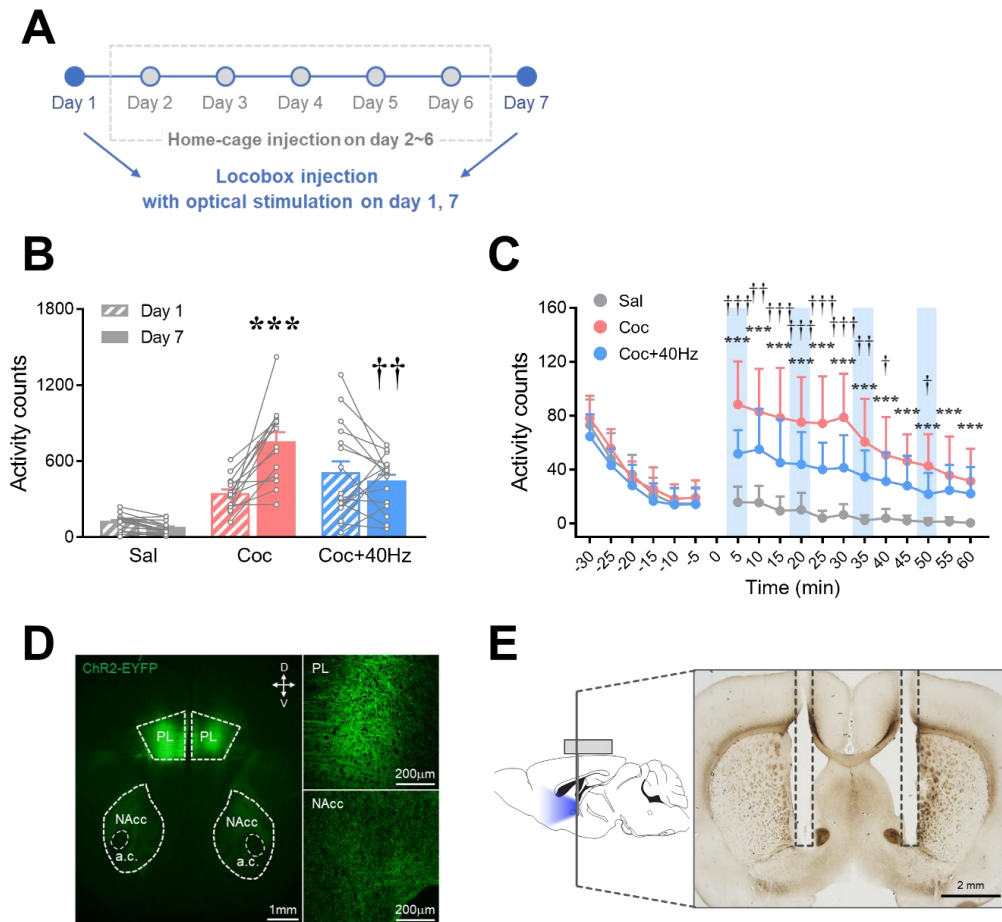


**Figure 2. The optogenetic stimulation of the PL-NAc core circuit inhibits cocaine-induced locomotor sensitization.** (A) Schematic diagram of experimental procedures of cocaine sensitization with optical stimulation. (B) Total locomotor activity counts measured during the 60 min test on days 1 and 7 after saline (gray), cocaine only (red), or cocaine with optical stimulation (blue). The sensitized locomotor activity by repeated cocaine administration was significantly suppressed by optical stimulation. \*\*\*  $p < 0.001$ , cocaine only group on day 7 compared to day 1. ††  $p < 0.01$ , cocaine with optical stimulation group compared with cocaine only group. (C) Time-course data shown as locomotor activity counts at 5 min intervals during the

30 min preceding (−30 ~ 0 min) and the 60 min following saline (gray), cocaine only (red), and cocaine with optical stimulation (blue). The sensitized locomotor activity was suppressed during optical stimulation delivered at 5, 20, 35, and 50 min (light blue bar). \*\*\*  $p < 0.001$ , cocaine only group compared to saline group. † $p < 0.05$ , †† $p < 0.01$ , ††† $p < 0.001$  cocaine with optical stimulation group compared with cocaine only group. Data are shown as mean + SEM. The numbers of rats for each group were as follows: saline (15), cocaine only (14), and cocaine with optical stimulation (16). **(D)** Epifluorescence image at low magnification (left), demonstrating ChR2-EYFP expression in both the PL and NAc core regions. At a higher magnification (right), it is more evident that ChR2-EYFP expressed well in cell body areas in the PL (upper right) and even at the axon terminal location in the NAc core (bottom right). **(E)** A representative bright-field image with probe tracks. Most tracks are found in the area that was aimed behind the NAc.

### **3. The optogenetic stimulation of the PL-NAc circuit suppresses the cocaine-induced c-Fos expression in the NAc core**

Based on the research that c-Fos is crucial in cocaine sensitization,<sup>41,79</sup> an immunofluorescence assay was performed to explore the effect of optical stimulation on c-Fos expression within the PL and NAc core. One-way ANOVA conducted on these data showed a significant difference between groups in the PL [ $F_{2,19} = 3.61$ ,  $p < 0.05$ ] and the NAc core [ $F_{2,19} = 3.59$ ,  $p < 0.05$ ]. Post-hoc Bonferroni t-test revealed significant increases in the ratio of c-Fos+ neurons to the total neurons in the PL ( $p < 0.05$ ) and the NAc core ( $p < 0.05$ ) by daily cocaine administrations. However, these increases were not reached to statistical significances in cocaine with optical stimulation groups (Figure 3A, B).

Because NAc-projecting PL neurons give rise to collaterals to striatum<sup>80</sup>, c-Fos expression in the striatum was also analyzed. One-way ANOVA conducted on these data showed a significant difference between groups [ $F_{2,19} = 6.985$ ,  $p < 0.01$ ]. Post-hoc Bonferroni t-test revealed significant increases in the c-Fos in both cocaine only ( $p < 0.01$ ) and cocaine with optical stimulation ( $p < 0.05$ ) groups (Figure 3C).

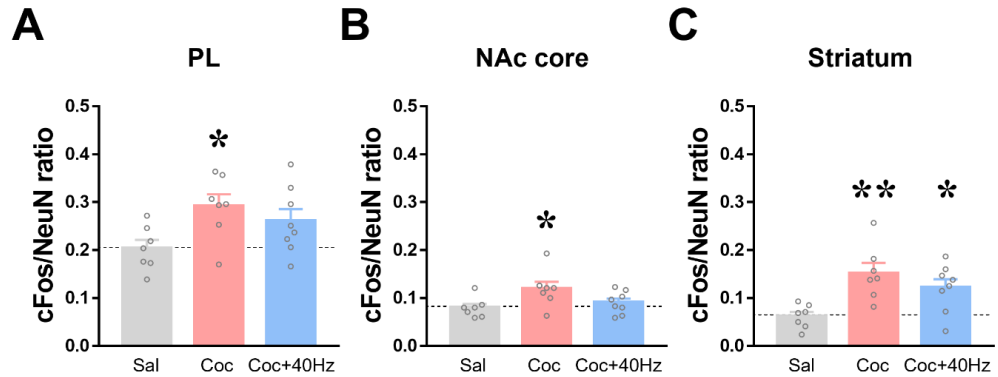


**Figure 3. The optogenetic stimulation of the PL-NAc core circuit reduced cocaine-induced c-Fos expression. (A, B)** The ratio of c-Fos+ neurons to the total neurons in the PL and the NAc core. The c-Fos+ neurons were significantly increased by seven daily cocaine administrations but these effects lost statistical significances with optical stimulation. **(C)** The c-Fos+ neurons in the striatum were also increased by seven daily cocaine administrations but not changed with optical stimulation. The numbers of rats used for each group were as follows: saline (7), cocaine only (7), and cocaine with optical stimulation (8). \* $p < 0.05$ , \*\*  $p < 0.01$ , significantly different to saline group. Data are shown as mean + SEM.

#### **4. Optogenetic stimulation of the PL-NAc circuit inhibits the increase in mushroom spine density induced by repeated cocaine exposures**

Based on the research that repeated cocaine exposures induce an increase of dendritic spine density in the NAc core,<sup>43</sup> it was examined whether the dendritic spine density was altered by optical stimulation. Rats were perfused after second optical stimulation on day 7 and the brain tissues were stained using the Golgi-Cox method to count dendritic spines in the NAc core (Figure 4, 5). Figure 4A shows a representative image of the Golgi-Cox-stained neurons and the dendrite in the NAc core obtained from confocal reflection microscopy.

Total spine density was not significantly different between the groups (Figure 4B). However, when analyzed by each spine subtype, a significant increase in mushroom spine density was observed in the cocaine group. One-way ANOVA conducted on these data showed a significant difference between groups in mushroom spine density [ $F_{2,11} = 5.402$ ,  $p < 0.05$ ], and post-hoc Bonferroni t-test revealed that the cocaine group had higher mushroom spine density than saline group ( $p < 0.05$ ). This increase of the mushroom spine density was not observed in cocaine with optical stimulation group (Figure 4E). No significant differences were found in other sub-types of spine densities (Figure 4C, D).

In addition to the density, head diameters and spine-lengths of each spine were also measured. One-way ANOVA conducted on these data showed a significant difference between groups [ $F_{2,11} = 5.268$ ,  $p < 0.05$ ] in head diameters of thin spines. Post-hoc Bonferroni t-test revealed that head diameters of thin spine were significantly decreased in cocaine with optical stimulation group compared with saline group ( $p < 0.05$ ) (Figure 5A). No statistical significances were found in head diameters in other sub-types of spine (Figure 5B, C). There were also no significant differences in spine-length in all sub-types of spine (Figure 5D-F).

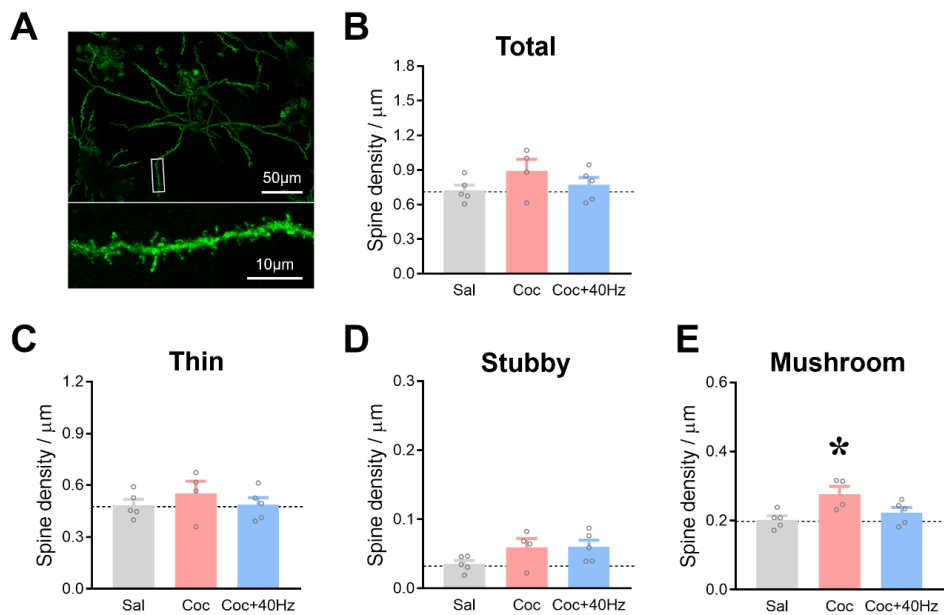


**Figure 4. Optogenetic stimulation of the PL-NAc core circuit suppressed the increase of mushroom spine density by cocaine.** (A) Representative images of confocal microscopy demonstrate Golgi-Cox-stained neurons in the NAc core (*top*, at low magnification) and spines on the dendrite marked as a white rectangle (*bottom*, at high magnification). (B-E) Mushroom spine density was significantly increased by repeated cocaine administration, whereas it was disappeared with optical stimulation. Total and other sub-types of spine densities in the NAc core were not different between the groups. The numbers of rats and neurons for each group were as follows: saline (5 rats), cocaine only (4 rats), and cocaine with optical stimulation (5 rats). 10 to 15 neurons were used per rat. \* $p < 0.05$ , significantly different to saline group. Data are shown as mean + SEM.

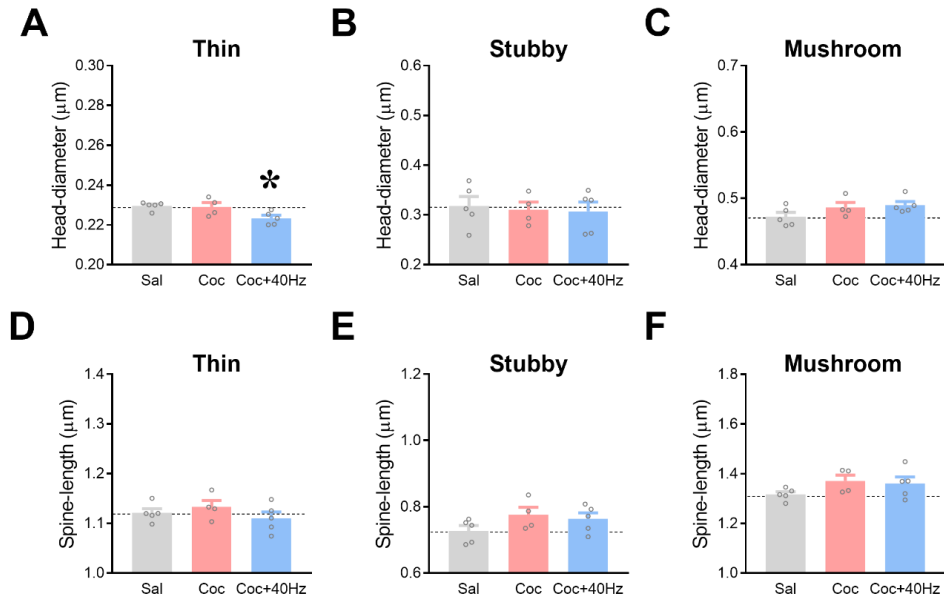


**Figure 5. Optogenetic stimulation of the PL-NAc core circuit reduced the head diameter in thin spine.** (A) Head diameter of thin spine was significantly decreased in cocaine with optical stimulation group compared with saline group. Neurons were 10 to 15 per rat and rats were 5 per group. \* $p < 0.05$ , significantly different to saline group. (B, C) No significant differences in head diameters were observed in other sub-types of spines. (D-F) The lengths of all sub-types of spine were not different between groups. Data are shown as mean + SEM.

## **5. Optogenetic stimulation of the PL-NAc core circuits increases rats' preference toward risky choice in the risk-averse group**

After a completion of rat gambling task (rGT) free choice sessions, rats were categorized into risk-averse and risk-seeking groups, depending on their stabilized preference for the P2 choice. They were further divided into EYFP or ChR2-EYFP subgroups and given bilateral infusions of a virus set. AAV expressing Cre-dependent EYFP or ChR2-EYFP was infused into the PL and retrograde AAV expressing Cre recombinase was infused into the NAc core. Simultaneously, the opto-device was also implanted on the rat skull, inserting the bilateral probes with  $\mu$ -ILED at the far posterior site of the NAc. Two weeks after the surgery, the rGT free choice sessions were re-performed to remind rats of their preference and the average choice scores for the last 3 days were used as a baseline of the preference (Recovery rGT). In the opto-rGT free choice sessions, optical stimulation was given 20 or 40 Hz blue lights during 5 sec of every inter-trial interval (ITI) for the first 7 days, and vice versa in a counter-balanced way for the second 7 days (Figure 6).

Figure 7 shows overall results of risky choice (choice of P3+P4 out of the total as a percent), which is an indicative of impulsive choice, in the risk-averse and the risk-seeking groups during the opto-rGT sessions with 20 or 40 Hz optical stimulation. When the risk-averse rats were given 20 Hz optical stimulation, they showed slight daily increases in the risky choice preference. Although these daily score data did not reach statistical significance, average score for the last 3 days showed a significant increase. Two-way repeated measure ANOVA conducted on these data revealed a significant effect of optical stimulation [ $F_{1,18} = 5.175$ ,  $p < 0.05$ ] and post-hoc Bonferroni t-test revealed a significant increase in the risky choice in the ChR2 group ( $p < 0.05$ ) (Figure 7A). When the risk-averse rats were given 40 Hz optical stimulation, they showed a higher magnitude of increase in the risky choice. Two-way ANOVA conducted on the time-course data showed a significant effect of optical stimulation

[ $F_{7,126} = 3.714$ ,  $p = 0.001$ ] and post-hoc Bonferroni t-test revealed that 40 Hz optical stimulation significantly increased ( $p < 0.05$ – $0.001$ ) daily risky choice scores with statistical significances on days of 3, 4, 6 and 7 compared to those from the recovery rGT. Two-way ANOVA conducted on the average score data showed a significant effect of optical stimulation [ $F_{1,18} = 6.549$ ,  $p < 0.05$ ] and post-hoc Bonferroni t-test revealed a significant increase in the risky choice in the ChR2 group ( $p < 0.01$ ) (Figure 7B). These effects were not observed in risk-seeking rats with any optical stimulations that were used (Figure 7C, D).

Preference scores (as percent of total) during the recovery rGT and the opto-rGT with 40 Hz optical stimulation are presented in Figure 8. The risk-averse rats expressing EYFP showed no difference in the preference scores (Figure 8A). However, the risk-averse rats expressing ChR2 altered their choice preference. Two-way ANOVA conducted on these data revealed multiple significant effects on choice [ $F_{3,30} = 71.959$ ,  $p < 0.001$ ] and choice  $\times$  optical stimulation [ $F_{3,30} = 5.049$ ,  $p < 0.001$ ]. Post-hoc Bonferroni t-test revealed a significant decrease in P2 choice ( $p < 0.01$ ) and an increase in P3 choice ( $p < 0.01$ ) (Figure 8B). The risk-seeking rats expressing EYFP or ChR2 showed no change in their choice preference (Figure 8C, D). These results show that optogenetic stimulation of the PL-NAc core circuit altered rats' preference toward risky options only in the risk-averse group.

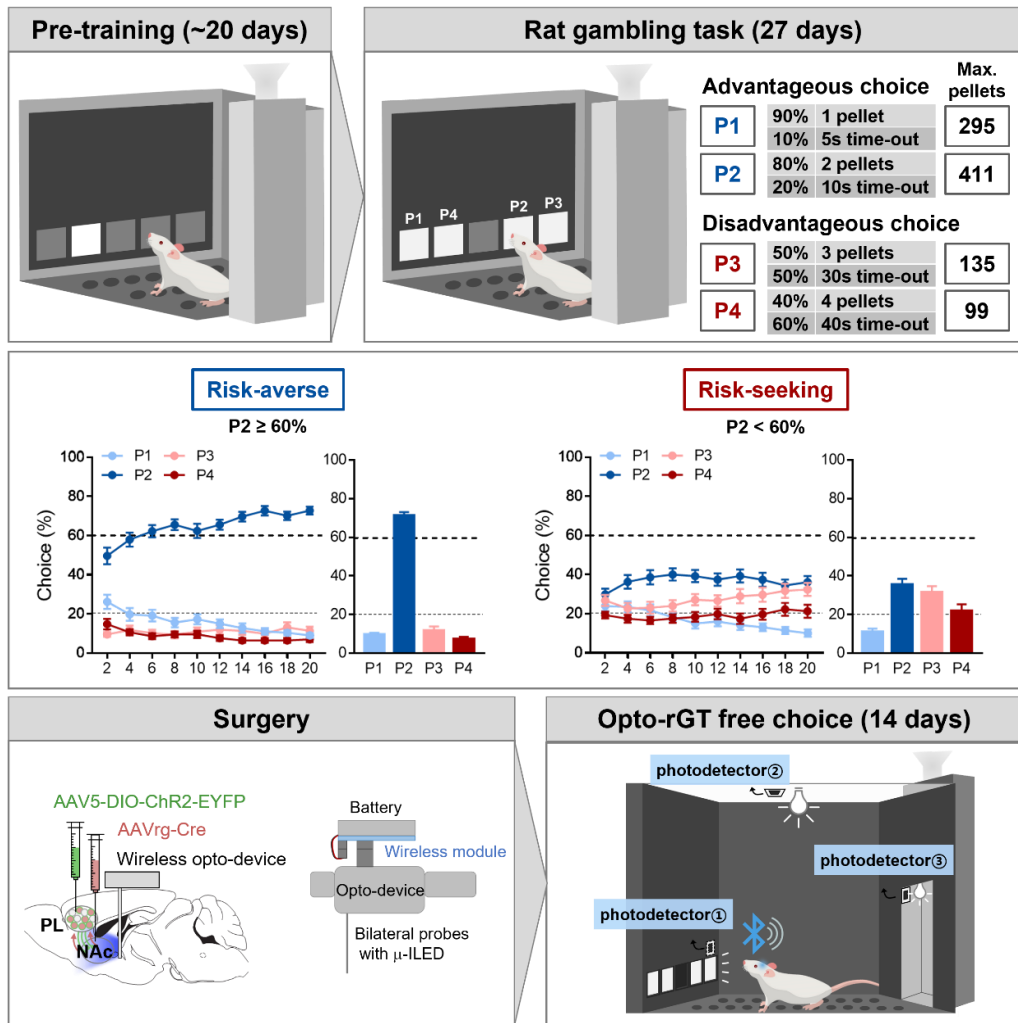


**Figure 6. Schematic illustrations of optogenetic experimental procedures in rat gambling task.** (Top) Schematic diagram of the rGT chamber. P1~P4 indicate the windows on the screen. The number of pellets as rewards and time-outs as punishments together with their corresponding probabilities are shown on the right. In addition, the hypothetical calculation of the maximum number of pellets that rats would obtain during the 30-minute trial is shown. (Middle) Rats were divided into the risk-averse and the risk-seeking groups according to their preference. Daily choice scores for 20 days of the rGT and the average scores for the last 3 days are presented.

(*Bottom, left*) Schematic illustrations show rat brain where virus and device were located and the opto-device with  $\mu$ -ILED probe connected with battery. (*Bottom, right*) A schematic illustration shows a wireless photodetector-based closed-loop optogenetic system in the rGT. Photodetectors were installed for detecting lights on the screen, house, and food-magazine. When all lights are off, a BLE MCU board connected with the photodetectors sends a LED-on signal to the wireless module. However, when any light is on, the board sends a LED-off signal.

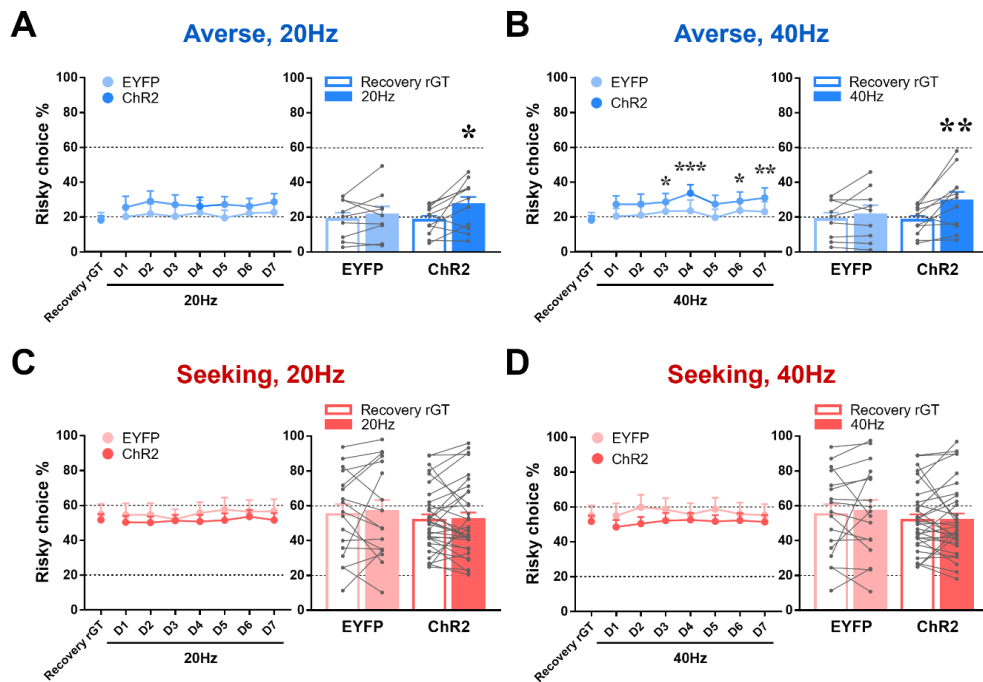


**Figure 7. The risk-averse rats’ preference for risky choice is increased by optical stimulation.** An average risky choice score for the last 3 days of the recovery rGT and daily scores during the opto-rGT with either 20 Hz or 40 Hz optical stimulation are shown in a time-course data. Average risky choice scores for the last 3 days of the recovery rGT and the opto-rGT are compared in a bar graph. **(A)** In the risk-averse rats, the opto-rGT with 20 Hz optical stimulation increased daily risky choice scores, and the average score for the last 3 days reached statistical significance. **(B)** When 40 Hz optical stimulation was delivered to the risk-averse rats, it increased daily risky choice scores with statistical significances on days of 3, 4, 6 and 7 compared to the those from the recovery rGT. **(C, D)**. No change of risky choice score was observed for the risk-seeking rats regardless of the stimulation frequency. \* $p < 0.05$ , \*\* $p < 0.01$ , \*\*\* $p < 0.001$ , comparison between the recovery rGT and the opto-rGT with either 20 Hz or 40 Hz optical stimulation. The numbers of rats for each group were as follows: averse-EYFP (9), averse-ChR2 (11), seeking-EYFP (17), seeking-ChR2 (32).

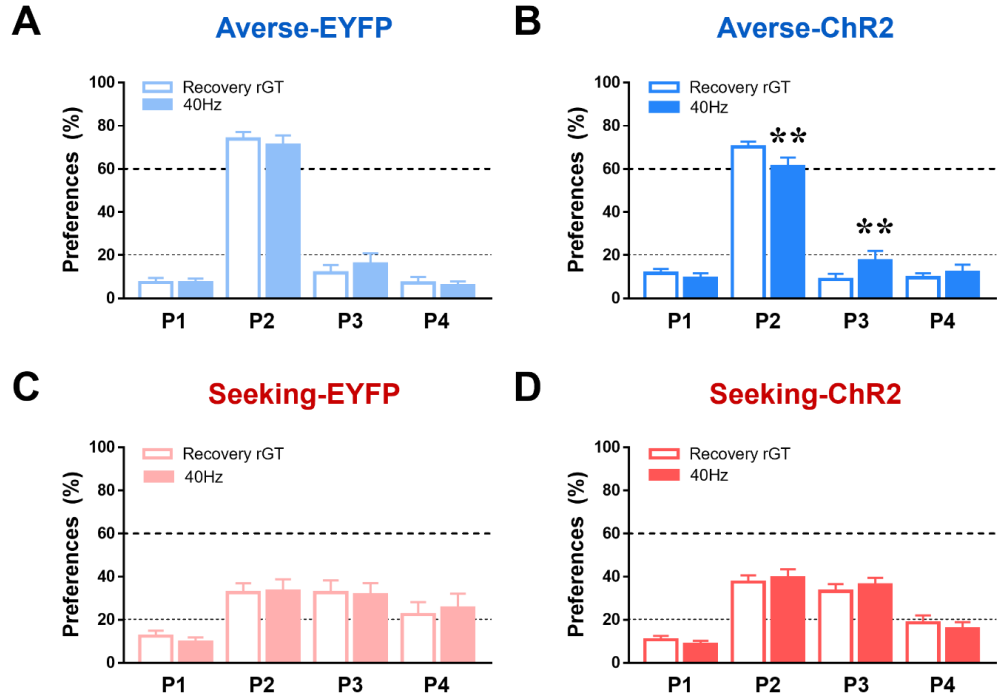


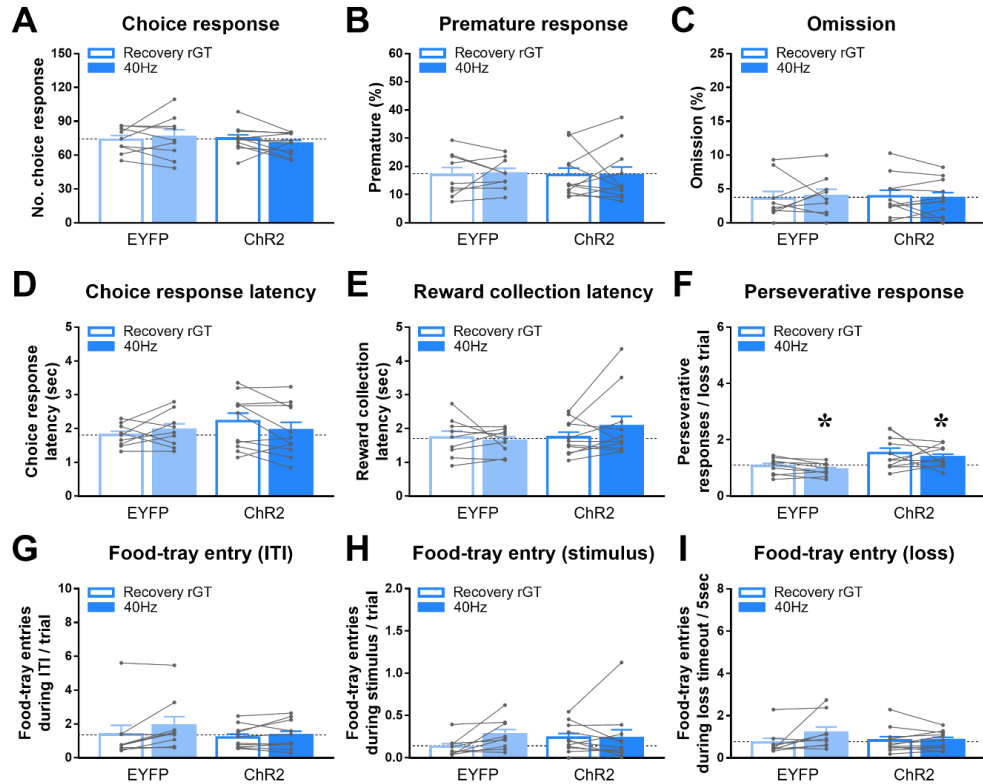
**Figure 8. The risk-averse rats' preference is shifted from the P2 to the P3 choice by 40 Hz optical stimulation.** The preference scores for each window (P1~P4) were obtained during the last 3 days of the recovery rGT and the opto-rGT. **(A)** Preference scores in the risk-averse rats expressing EYFP were not changed by 40 Hz optical stimulation. **(B)** Significant decrease in the P2 choice and increase in the P3 choice were observed in the risk-averse rats expressing ChR2-EYFP by 40 Hz optical stimulation. **(C, D)** Preference scores were not changed in the risk-seeking rats expressing either EYFP or ChR2-EYFP. \*\* $p < 0.01$ , compared to the recovery rGT. The numbers of rats for each group are as follows: averse-EYFP (9), averse-ChR2 (11), seeking-EYFP (17), seeking-ChR2 (32).

## 6. The effects of the optical stimulation on behavioral parameters related with rGT appeared to vary according to risk preference

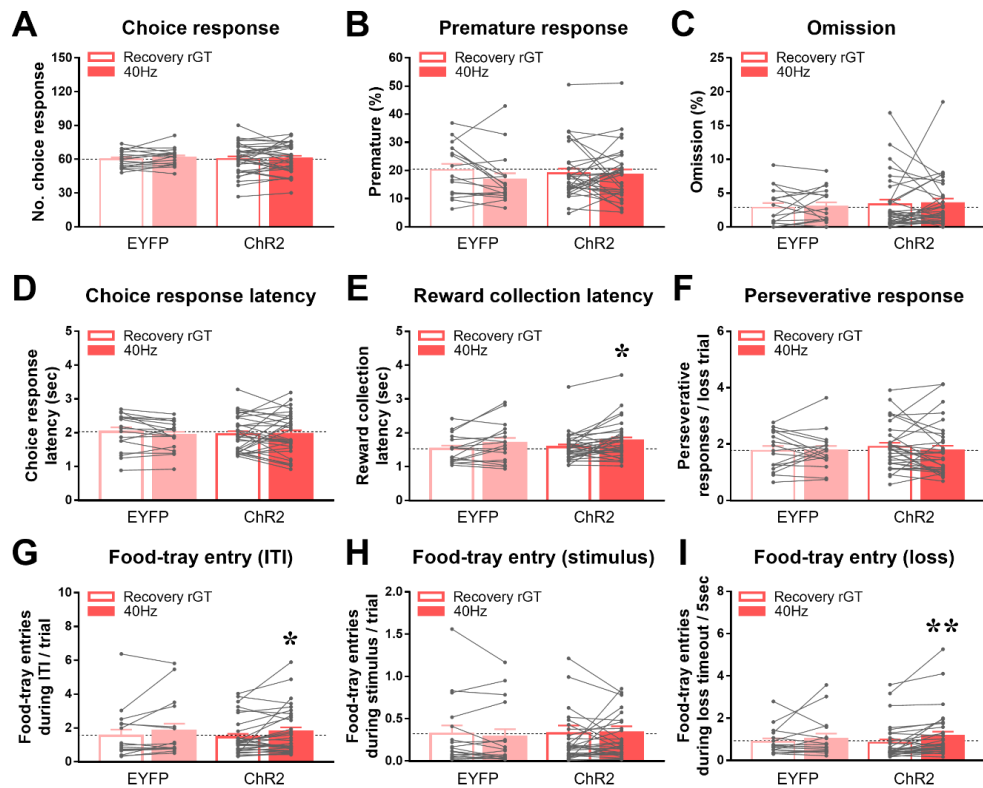
Several behavioral parameters related with rGT<sup>55,81</sup> during the recovery and 40 Hz optical stimulation were analyzed. Figure 9 shows the behavioral parameters in the risk-averse group. The number of choice response and the omission score were not altered by the optical stimulation, indicating that rats' attention to the task was not affected by the optical stimulation (Figure 9A, C). The optical stimulation also did not alter premature score, indicating that impulsive action was not changed (Figure 9B). Latencies to choice response and reward collection were not changed by optical stimulation (Figure 9D, E). Among repeated behaviors including perseverative response and food-tray entries (Figure 9F-I), the perseverative response per loss trial was significantly decreased during optical stimulation. However, this effect was observed not only in the ChR2 group but also in the EYFP group, which had no light-sensitive channel. Two-way ANOVA conducted on these data showed a significant effect of virus [ $F_{1,18} = 10.762$ ,  $P < 0.01$ ] and post-hoc Bonferroni t-test revealed a significant decrease in the perseverative response in both the EYFP ( $p < 0.05$ ) and the ChR2 groups ( $p < 0.05$ ) (Figure 9F).

Figure 10 demonstrates the behavioral parameters in the risk-seeking group, which shows a distinct pattern from those in the risk-averse rats. Reward collection latency and food-tray entries (during both ITI and loss timeout) were increased in the ChR2 group by optical stimulation. Two-way ANOVA conducted on these data showed a significant effect of optical stimulation in reward collection latency [ $F_{1,47} = 9.886$ ,  $p < 0.05$ ], food-tray entry during ITI [ $F_{1,47} = 7.157$ ,  $p < 0.05$ ], and food-tray entry during loss timeout time [ $F_{1,47} = 7.136$ ,  $p < 0.05$ ]. Post-hoc Bonferroni t-tests showed a significant increase in reward collection latency ( $p < 0.05$ ), food-tray entry during ITI ( $p < 0.05$ ) and food-tray entry during loss timeout time ( $p < 0.01$ ) in the ChR2 group (Figure 10E, G, I). These results show that the optogenetic stimulation of

the PL-NAc core circuit differentially affected rGT-related behavioral parameters in the risk-seeking group from the risk-averse group.



**Figure 9.** Comparison of behavioral parameters related with rGT between the recovery test and the opto-stimulation in the risk-averse rats. (A-C) Trial-related parameters such as choice response, premature response, and omission, were not changed by optical stimulation. (D-E) Latencies to choice response and reward collection were not changed by optical stimulation. (F-I) Among repeated behaviors including perseverative response per loss trial, food-tray entries during ITI, stimulus duration and loss timeout time, the perseverative response was significantly decreased in the risk-averse rats expressing either EYFP or ChR2-EYFP. \* $p < 0.05$ , comparison between the recovery rGT and the opto-rGT. The numbers of rats for each group are as follows: averse-EYFP (9), averse-ChR2 (11).



**Figure 10.** Comparison of behavioral parameters related with rGT between the recovery test and the opto-stimulation in the risk-seeking rats. (A-C) Trial-related parameters such as choice response, premature response, and omission, were not changed by optical stimulation. (D-E) Among latencies to choice response and reward collection, reward collection latency was significantly increased in the risk-seeking rats expressing ChR2-EYFP. (F-I) Among repeated behaviors, food-tray entries during ITI and loss timeout time were significantly increased in the risk-seeking rats expressing ChR2-EYFP. Perseverative response per loss trial and food-tray entries during stimulus duration were not changed. \* $p < 0.05$ , \*\* $< 0.01$ , comparison between the recovery rGT and the opto-rGT. The numbers of rats for each group are as follows: seeking-EYFP (17), seeking-ChR2 (32).

## IV. DISCUSSION

In this thesis, I utilized wireless optogenetic techniques to precisely manipulate a specific neural circuit with high temporal resolution. The neural probes of the opto-device were coated with polydimethylsiloxane (PDMS) and parylene C bilayer for biocompatibility, chemical inertness, and waterproofing.<sup>82</sup> A wireless operating system with a customized smartphone app was previously developed,<sup>72</sup> and it was improved to automatically deliver LED on/off signals in this study. A photodetector-based wireless closed-loop system was also established for automated delivery of optical stimulation only during decision-making. Using these techniques, the roles of the PL-NAc core circuit in animal models of drug and gambling addictions were precisely investigated.

The present findings demonstrated that the optogenetic stimulation of the PL-NAc core circuit strongly inhibited cocaine-induced locomotor sensitization. As expected, rats administered cocaine showed sensitized locomotor activity. However, those concurrently delivered with optical stimulation failed to show sensitized locomotor activity when comparing day 7 to day 1, and this effect was evident during every time point of optical stimulation on day 7 (Figure 2B, C). The inhibition of sensitized locomotor activity was not attributable to decreased basal locomotor activity because the optogenetic stimulation had no effect on basal locomotor activity without cocaine. Neuronal activity within the NAc is known to involve mediating many drug-related behaviors including behavioral sensitization.<sup>74</sup> For example, cocaine-induced locomotor sensitization was accompanied by sensitized c-Fos expression in the NAc.<sup>41</sup> In the present study, optogenetic stimulation of the PL-NAc core circuit suppressed the increase in c-Fos expression induced by cocaine in the PL and NAc core, suggesting that these effects might contribute to inhibiting the expression of locomotor sensitization by cocaine. It was confirmed that the optogenetic stimulation selectively regulated the PL-NAc core activities because the stimulation did not affect c-Fos

expression in the striatum, to which the NAc-projecting PL neurons give rise to collaterals.

It is well established that psychoactive stimulants induce structural plasticity of dendritic spines in the NAc, and this alteration is crucial for development of drug addiction.<sup>45,83</sup> For example, repeated administration of cocaine or amphetamine significantly increased the dendritic spine density in the NAc.<sup>44,84</sup> Among spine subtypes, mushroom spines are considered the most stable and functional. Mushroom spines have more glutamate receptors in larger postsynaptic densities, which make more functional synapses.<sup>85</sup> The present study demonstrated that the increase in mushroom spine density induced by cocaine was diminished by the optogenetic stimulation of the PL-NAc core (Figure 4E). The reduced density of mushroom spines possessing a large head diameter may attenuate the postsynaptic properties of the NAc because the excitatory glutamatergic projections from the mPFC mainly synapse onto the heads of dendritic spines in the NAc.<sup>86</sup>

c-Fos expression and neuronal activation are known to require strong and persistent synaptic activity.<sup>87,88</sup> Furthermore, while cocaine administration increased mushroom spine density, a further increase in mushroom spine density was observed in c-Fos+ neurons.<sup>89</sup> Thus, it may be possible that the concurrent reduction of mushroom spine density and c-Fos expression in the NAc core by optogenetic stimulation of the PL-NAc core circuit contributed to weakening of the neuronal activity at this site, thereby resulting in the inhibition of the expression of behavioral sensitization.

How the optogenetic stimulation of the PL-NAc core altered the mushroom spine density in the NAc core remains unclear. Interestingly, there was a report that chemically or optogenetically evoked long-term depression (LTD) eliminated the dendritic spines, particularly the mushroom spines.<sup>90,91</sup> Furthermore, optogenetic stimulation of IL-NAc shell was reported to induce robust LTD of dopamine receptor

type-1 (D1R)-expressing neurons in the NAc shell, thus abolishing the sensitized locomotor response by cocaine. Even a relatively mild opto-stimulation protocol (4-ms pulses at 1 Hz or 12 Hz for 10 minutes) was shown to induce LTD of postsynaptic neurons.<sup>70,92</sup> Therefore, it may be possible that the opto-stimulation conditions used in the present study (10-ms pulses at 40 Hz for 5 min stimulation, 30 s on/off, with a 10-min light free interval throughout 60 min) could induce LTD of the postsynaptic neurons in the NAc core, which may contribute to eliminating the mushroom spines increased by cocaine.

In the rGT experiment, optical stimulation was delivered during every ITI, in which rats may be deliberating about their choices prior to decision-making. Optogenetic stimulation of the PL-NAc core made a differential effect on the rats' impulsive choices according to their pre-categorized choice preference; only the risk-averse group increased impulsive choice with optical stimulation. This effect was more evident with optical stimulation of 40 Hz than with 20 Hz, indicating that the higher frequency of optical stimulation was more effective in driving rats' preferences toward risky options (Figure 7A, B). This increased preference for a risky choice resulted mostly from the decreased P2 choice and the increased P3 choice (Figure 8B). Interestingly, impulsive action (i.e., premature) was not changed by optical stimulation, suggesting that the PL-NAc core circuit may selectively contribute to mediating impulsive choice. Most other rGT-related behavioral parameters were not changed by optical stimulation, but the perseverative response was slightly decreased after opto-stimulation in both the EYFP and ChR2 groups. There was less chance that this effect would contribute to the altered preference for the risky choice because the risk-averse rats expressing EYFP did not shift their choice preference (Figure 9F).

The risk-seeking group, unlike the risk-averse group, did not change their preference with the same optical stimulation (Figure 7C, D, and Figure 8D). Interestingly, however, they exhibited changes in some rGT-related behavioral

parameters (Figure 10E, G and I). With optical stimulation, they showed higher reward collection latency compared to the baseline, which is indicative that they had less interest in the reward. In addition, they showed the increased entries to the food tray (during both ITI and loss time-out), which may be an indicator that they were more driven to initiate the next trials. These results suggest that the PL-NAc core in the risk-seeking rats may contribute to motivation for playing gambling itself rather than obtaining the reward, which makes them different from risk-averse rats.

These findings imply that the PL-NAc core may have different neuronal properties that provoke distinct motivation depending on pre-categorized choice preferences. For example, it is known that impulsive choices were correlated or associated with the neuronal activity in the PL and NAc core.<sup>64-66,93</sup> Further, it has been recently shown that transcriptome profiles are differentially expressed in the mPFC and NAc depending on rats' choice preference toward risk in the rGT, which may underlie differential neural properties within the PL-NAc core.<sup>94</sup> It would be interesting in the future to directly compare the neuronal activity within the PL-NAc core during decision-making in the risk-averse and risk-seeking rats.

Interestingly, there are reports showing that different populations of neurons encoding reward or punishment distinctively exist in the PL. For example, it has been reported that NAc-projecting neurons in the mPFC can be separated depending on their activities responding to a reward or foot-shock punishment, which suggests that the individual neurons could differentially encode either the reward or the punishment.<sup>95</sup> Further, risky choices are more likely driven by hyposensitivity to punishment.<sup>96</sup> Thus, it is possible that the population of punishment-active neurons in the PL-NAc core circuit and their activity patterns may differentially exist according to the risk preference in the rGT, which may contribute to differential responses between risk-averse and risk-seeking groups.

It is worth mentioning that, in my thesis, the change in the impulsive choice was

observed by optical stimulation during ITI. It will be interesting to determine what effects will appear with optical stimulation during other phases of the rGT (e.g., reward delivery, timeout punishment, or ITI specifically following either a reward or punishment).

It has been shown that both cocaine addicts and cocaine-sensitized rats showed a strong preference for risky options,<sup>56,97,98</sup> and also risk-preferring rats showed heightened cocaine-seeking responses and greater cue-induced craving.<sup>99</sup> The present study demonstrated that the frontostriatal circuitry, specifically the PL-NAc core circuit, has a regulatory role in mediating both the craving in cocaine sensitization and decision-making in the rGT (Figure 11), which suggest that this circuit could be considered as an important common target mediating two distinctive clinical features. Further, this study may provide insight into a possible link between drug and behavioral addictions, thereby lead to a novel treatment strategy in the future.

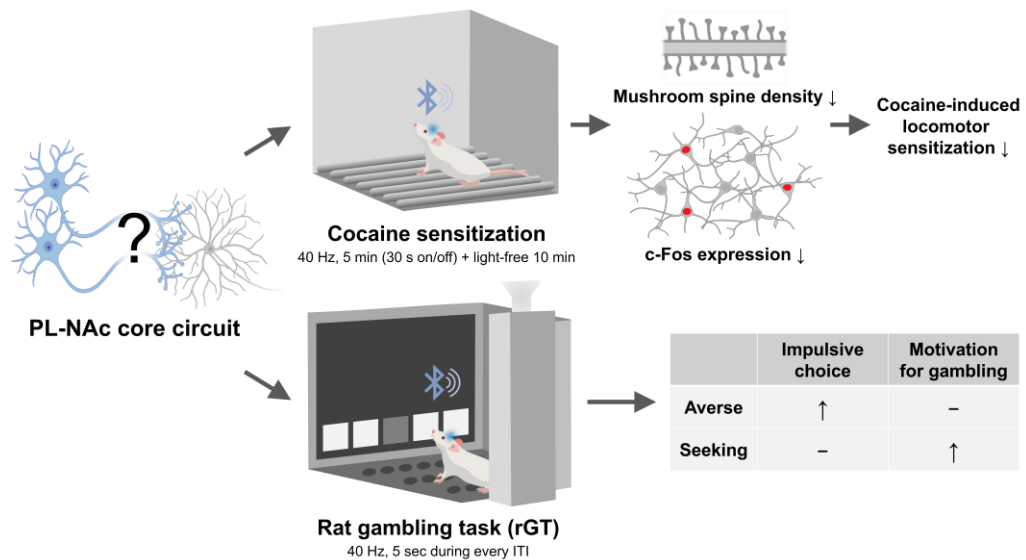


**Figure 11. An overview of the effects of optogenetic manipulation of the PL-NAc core circuit on cocaine sensitization and gambling-related behaviors in rGT.** It was examined how the optogenetic modulation of the PL-NAc core circuit influenced the behavioral sensitization and impulsive decision-making in rGT. Optogenetic stimulation of the PL-NAc core significantly inhibited cocaine-induced locomotor sensitization by reducing the increase in c-Fos expression and mushroom spine density in the NAc core. Further, it also increased impulsive choices in risk-averse group of rats, whereas it increased reward collection latency and food-tray entries in risk-seeking group, which may indicate higher motivation for playing gambling. Created with Biorender.com.

## V. CONCLUSION

In this study, the roles of the PL-NAc core circuit in animal models of drug and gambling addictions were examined using wireless optogenetics that minimizes human intervention and restriction of animals' movement. This is the first study, to my knowledge, to demonstrate that optogenetic manipulation of the PL-NAc core circuit can inhibit the expression of cocaine-induced behavioral sensitization by decreasing mushroom spine density and c-Fos expression induced by cocaine in the NAc core. In addition, the present study first time conducted optogenetic manipulation of the PL-NAc core circuit immediately prior to decision-making behaviors in the rGT. The PL-NAc core stimulated with light differentially contributed to rats' impulsive choices and rGT-related behavioral parameters according to their risk preference. These findings suggestively place the PL-NAc core circuit as a common neural substrate that may mediate craving and decision-making characteristically appeared in both drug and gambling addictions.

## REFERENCE

1. Everitt BJ, Robbins TW. Drug Addiction: Updating Actions to Habits to Compulsions Ten Years On. *Annu Rev Psychol* 2016;67:23-50.
2. Meyer PJ, King CP, Ferrario CR. Motivational Processes Underlying Substance Abuse Disorder. *Curr Top Behav Neurosci* 2016;27:473-506.
3. Potenza MN. Should addictive disorders include non-substance-related conditions? *Addiction* 2006;101:142-51.
4. Karim R, Chaudhri P. Behavioral addictions: an overview. *J Psychoactive Drugs* 2012;44:5-17.
5. Petry NM, Stinson FS, Grant BF. Comorbidity of DSM-IV pathological gambling and other psychiatric disorders: results from the National Epidemiologic Survey on Alcohol and Related Conditions. *J Clin Psychiatry* 2005;66:564-74.
6. Grant JE, Potenza MN, Weinstein A, Gorelick DA. Introduction to behavioral addictions. *Am J Drug Alcohol Abuse* 2010;36:233-41.
7. Na E, Lee H, Choi I, Kim DJ. Comorbidity of Internet gaming disorder and alcohol use disorder: A focus on clinical characteristics and gaming patterns. *Am J Addict* 2017;26:326-34.
8. Kovács I, Demeter I, Janka Z, Demetrovics Z, Maraz A, Andó B. Different aspects of impulsivity in chronic alcohol use disorder with and without comorbid problem gambling. *PLoS One* 2020;15:e0227645.
9. Everitt BJ, Robbins TW. Neural systems of reinforcement for drug addiction: from actions to habits to compulsion. *Nat Neurosci* 2005;8:1481-9.
10. Koob GF, Volkow ND. Neurobiology of addiction: a neurocircuitry analysis. *Lancet Psychiatry* 2016;3:760-73.
11. Berridge KC. From prediction error to incentive salience: mesolimbic computation of reward motivation. *Eur J Neurosci* 2012;35:1124-43.

12. Sugam JA, Day JJ, Wightman RM, Carelli RM. Phasic nucleus accumbens dopamine encodes risk-based decision-making behavior. *Biol Psychiatry* 2012;71:199-205.
13. Groenewegen HJ, Wright CI, Beijer AV, Voorn P. Convergence and segregation of ventral striatal inputs and outputs. *Ann N Y Acad Sci* 1999;877:49-63.
14. Goldstein RZ, Volkow ND. Dysfunction of the prefrontal cortex in addiction: neuroimaging findings and clinical implications. *Nat Rev Neurosci* 2011;12:652-69.
15. Feil J, Sheppard D, Fitzgerald PB, Yucel M, Lubman DI, Bradshaw JL. Addiction, compulsive drug seeking, and the role of frontostriatal mechanisms in regulating inhibitory control. *Neurosci Biobehav Rev* 2010;35:248-75.
16. Breiter HC, Gollub RL, Weisskoff RM, Kennedy DN, Makris N, Berke JD, et al. Acute effects of cocaine on human brain activity and emotion. *Neuron* 1997;19:591-611.
17. Risinger RC, Salmeron BJ, Ross TJ, Amen SL, Sanfilippo M, Hoffmann RG, et al. Neural correlates of high and craving during cocaine self-administration using BOLD fMRI. *Neuroimage* 2005;26:1097-108.
18. Kohno M, Morales AM, Ghahremani DG, Helleman G, London ED. Risky decision making, prefrontal cortex, and mesocorticolimbic functional connectivity in methamphetamine dependence. *JAMA Psychiatry* 2014;71:812-20.
19. Clark L. Disordered gambling: the evolving concept of behavioral addiction. *Ann N Y Acad Sci* 2014;1327:46-61.
20. Weinstein AM. An Update Overview on Brain Imaging Studies of Internet Gaming Disorder. *Front Psychiatry* 2017;8:185.
21. Park SQ, Kahnt T, Beck A, Cohen MX, Dolan RJ, Wrase J, et al. Prefrontal cortex fails to learn from reward prediction errors in alcohol dependence. *J Neurosci* 2010;30:7749-53.

22. Wilcox CE, Teshiba TM, Merideth F, Ling J, Mayer AR. Enhanced cue reactivity and fronto-striatal functional connectivity in cocaine use disorders. *Drug Alcohol Depend* 2011;115:137-44.
23. Koehler S, Ovadia-Caro S, van der Meer E, Villringer A, Heinz A, Romanczuk-Seiferth N, et al. Increased functional connectivity between prefrontal cortex and reward system in pathological gambling. *PLoS One* 2013;8:e84565.
24. Becker A, Kirsch M, Gerchen MF, Kiefer F, Kirsch P. Striatal activation and frontostriatal connectivity during non-drug reward anticipation in alcohol dependence. *Addict Biol* 2017;22:833-43.
25. Yuan K, Zhao M, Yu D, Manza P, Volkow ND, Wang GJ, et al. Striato-cortical tracts predict 12-h abstinence-induced lapse in smokers. *Neuropsychopharmacology* 2018;43:2452-8.
26. Dong H, Wang M, Zhang J, Hu Y, Potenza MN, Dong GH. Reduced frontostriatal functional connectivity and associations with severity of Internet gaming disorder. *Addict Biol* 2021;26:e12985.
27. Potenza MN, Balodis IM, Franco CA, Bullock S, Xu J, Chung T, et al. Neurobiological considerations in understanding behavioral treatments for pathological gambling. *Psychol Addict Behav* 2013;27:380-92.
28. Yao YW, Zhang JT, Fang XY, Liu L, Potenza MN. Reward-related decision-making deficits in internet gaming disorder: a systematic review and meta-analysis. *Addiction* 2022;117:19-32.
29. Bechara A, Dolan S, Denburg N, Hindes A, Anderson SW, Nathan PE. Decision-making deficits, linked to a dysfunctional ventromedial prefrontal cortex, revealed in alcohol and stimulant abusers. *Neuropsychologia* 2001;39:376-89.
30. Tanabe J, Thompson L, Claus E, Dalwani M, Hutchison K, Banich MT. Prefrontal cortex activity is reduced in gambling and nongambling substance users during decision-making. *Hum Brain Mapp* 2007;28:1276-86.

31. Bickel WK, Jarmolowicz DP, Mueller ET, Koffarnus MN, Gatchalian KM. Excessive discounting of delayed reinforcers as a trans-disease process contributing to addiction and other disease-related vulnerabilities: emerging evidence. *Pharmacol Ther* 2012;134:287-97.
32. Dong G, Hu Y, Lin X, Lu Q. What makes Internet addicts continue playing online even when faced by severe negative consequences? Possible explanations from an fMRI study. *Biol Psychol* 2013;94:282-9.
33. Dong G, Potenza MN. Risk-taking and risky decision-making in Internet gaming disorder: Implications regarding online gaming in the setting of negative consequences. *J Psychiatr Res* 2016;73:1-8.
34. Liu L, Xue G, Potenza MN, Zhang JT, Yao YW, Xia CC, et al. Dissociable neural processes during risky decision-making in individuals with Internet-gaming disorder. *Neuroimage Clin* 2017;14:741-9.
35. Potenza MN. The importance of animal models of decision making, gambling, and related behaviors: implications for translational research in addiction. *Neuropsychopharmacology* 2009;34:2623-4.
36. Robinson TE, Berridge KC. The neural basis of drug craving: an incentive-sensitization theory of addiction. *Brain Res Brain Res Rev* 1993;18:247-91.
37. Robinson TE, Berridge KC. Review. The incentive sensitization theory of addiction: some current issues. *Philos Trans R Soc Lond B Biol Sci* 2008;363:3137-46.
38. Zhang Y, Loonam TM, Noailles PA, Angulo JA. Comparison of cocaine- and methamphetamine-evoked dopamine and glutamate overflow in somatodendritic and terminal field regions of the rat brain during acute, chronic, and early withdrawal conditions. *Ann N Y Acad Sci* 2001;937:93-120.
39. Everitt BJ, Wolf ME. Psychomotor stimulant addiction: a neural systems perspective. *J Neurosci* 2002;22:3312-20.

40. Uslaner J, Badiani A, Day HE, Watson SJ, Akil H, Robinson TE. Environmental context modulates the ability of cocaine and amphetamine to induce c-fos mRNA expression in the neocortex, caudate nucleus, and nucleus accumbens. *Brain Res* 2001;920:106-16.
41. Hope BT, Simmons DE, Mitchell TB, Kreuter JD, Mattson BJ. Cocaine-induced locomotor activity and Fos expression in nucleus accumbens are sensitized for 6 months after repeated cocaine administration outside the home cage. *Eur J Neurosci* 2006;24:867-75.
42. Fanous S, Lacagnina MJ, Nikulina EM, Hammer RP, Jr. Sensitized activation of Fos and brain-derived neurotrophic factor in the medial prefrontal cortex and ventral tegmental area accompanies behavioral sensitization to amphetamine. *Neuropharmacology* 2011;61:558-64.
43. Robinson TE, Kolb B. Structural plasticity associated with exposure to drugs of abuse. *Neuropharmacology* 2004;47 Suppl 1:33-46.
44. Lee KW, Kim Y, Kim AM, Helmin K, Nairn AC, Greengard P. Cocaine-induced dendritic spine formation in D1 and D2 dopamine receptor-containing medium spiny neurons in nucleus accumbens. *Proc Natl Acad Sci USA* 2006;103:3399-404.
45. Golden SA, Russo SJ. Mechanisms of psychostimulant-induced structural plasticity. *Cold Spring Harb Perspect Med* 2012;2.
46. Sesack SR, Deutch AY, Roth RH, Bunney BS. Topographical organization of the efferent projections of the medial prefrontal cortex in the rat: an anterograde tract-tracing study with *Phaseolus vulgaris* leucoagglutinin. *J Comp Neurol* 1989;290:213-42.
47. Voorn P, Vanderschuren LJ, Groenewegen HJ, Robbins TW, Pennartz CM. Putting a spin on the dorsal-ventral divide of the striatum. *Trends Neurosci* 2004;27:468-74.
48. Sepulveda-Orengo MT, Healey KL, Kim R, Auriemma AC, Rojas J, Woronoff N, et al. Riluzole Impairs Cocaine Reinstatement and Restores Adaptations in

- Intrinsic Excitability and GLT-1 Expression. *Neuropsychopharmacology* 2018;43:1212-23.
49. McGlinchey EM, James MH, Mahler SV, Pantazis C, Aston-Jones G. Prelimbic to Accumbens Core Pathway Is Recruited in a Dopamine-Dependent Manner to Drive Cued Reinstatement of Cocaine Seeking. *J Neurosci* 2016;36:8700-11.
  50. Siemsen BM, Barry SM, Vollmer KM, Green LM, Brock AG, Westphal AM, et al. A Subset of Nucleus Accumbens Neurons Receiving Dense and Functional Prelimbic Cortical Input Are Required for Cocaine Seeking. *Front Cell Neurosci* 2022;16:844243.
  51. Augur IF, Wyckoff AR, Aston-Jones G, Kalivas PW, Peters J. Chemogenetic Activation of an Extinction Neural Circuit Reduces Cue-Induced Reinstatement of Cocaine Seeking. *J Neurosci* 2016;36:10174-80.
  52. Winstanley CA, Clark L. Translational Models of Gambling-Related Decision-Making. *Curr Top Behav Neurosci* 2016;28:93-120.
  53. Nautiyal KM, Okuda M, Hen R, Blanco C. Gambling disorder: an integrative review of animal and human studies. *Ann N Y Acad Sci* 2017;1394:106-27.
  54. de Visser L, Homberg JR, Mitsogiannis M, Zeeb FD, Rivalan M, Fitoussi A, et al. Rodent versions of the iowa gambling task: opportunities and challenges for the understanding of decision-making. *Front Neurosci* 2011;5:109.
  55. Zeeb FD, Robbins TW, Winstanley CA. Serotonergic and dopaminergic modulation of gambling behavior as assessed using a novel rat gambling task. *Neuropsychopharmacology* 2009;34:2329-43.
  56. Kim WY, Cho BR, Kwak MJ, Kim JH. Interaction between trait and housing condition produces differential decision-making toward risk choice in a rat gambling task. *Sci Rep* 2017;7:5718.
  57. Bechara A, Damasio AR, Damasio H, Anderson SW. Insensitivity to future consequences following damage to human prefrontal cortex. *Cognition* 1994;50:7-15.

58. Bechara A, Damasio H, Damasio AR, Lee GP. Different contributions of the human amygdala and ventromedial prefrontal cortex to decision-making. *J Neurosci* 1999;19:5473-81.
59. Whitlow CT, Liguori A, Livengood LB, Hart SL, Mussat-Whitlow BJ, Lamborn CM, et al. Long-term heavy marijuana users make costly decisions on a gambling task. *Drug Alcohol Depend* 2004;76:107-11.
60. Brevers D, Cleeremans A, Goudriaan AE, Bechara A, Kornreich C, Verbanck P, et al. Decision making under ambiguity but not under risk is related to problem gambling severity. *Psychiatry Res* 2012;200:568-74.
61. Mallorquí-Bagué N, Fagundo AB, Jimenez-Murcia S, de la Torre R, Baños RM, Botella C, et al. Decision Making Impairment: A Shared Vulnerability in Obesity, Gambling Disorder and Substance Use Disorders? *PLoS One* 2016;11:e0163901.
62. Jiang C, Li C, Zhou H, Zhou Z. Individuals with internet gaming disorder have similar neurocognitive impairments and social cognitive dysfunctions as methamphetamine-dependent patients. *Adicciones* 2020;0:1342.
63. Ferland JN, Hynes TJ, Hounjet CD, Lindenbach D, Vonder Haar C, Adams WK, et al. Prior Exposure to Salient Win-Paired Cues in a Rat Gambling Task Increases Sensitivity to Cocaine Self-Administration and Suppresses Dopamine Efflux in Nucleus Accumbens: Support for the Reward Deficiency Hypothesis of Addiction. *J Neurosci* 2019;39:1842-54.
64. de Visser L, Baars AM, Lavrijsen M, van der Weerd CM, van den Bos R. Decision-making performance is related to levels of anxiety and differential recruitment of frontostriatal areas in male rats. *Neuroscience* 2011;184:97-106.
65. van Hasselt FN, de Visser L, Tieskens JM, Cornelisse S, Baars AM, Lavrijsen M, et al. Individual variations in maternal care early in life correlate with later life decision-making and c-fos expression in prefrontal subregions of rats. *PLoS One* 2012;7:e37820.

66. St Onge JR, Floresco SB. Prefrontal cortical contribution to risk-based decision making. *Cereb Cortex* 2010;20:1816-28.
67. Zeeb FD, Baarendse PJ, Vanderschuren LJ, Winstanley CA. Inactivation of the prelimbic or infralimbic cortex impairs decision-making in the rat gambling task. *Psychopharmacology (Berl)* 2015;232:4481-91.
68. Yizhar O, Fenno LE, Davidson TJ, Mogri M, Deisseroth K. Optogenetics in neural systems. *Neuron* 2011;71:9-34.
69. Zalocusky KA, Ramakrishnan C, Lerner TN, Davidson TJ, Knutson B, Deisseroth K. Nucleus accumbens D2R cells signal prior outcomes and control risky decision-making. *Nature* 2016;531:642-6.
70. Pascoli V, Turiault M, Luscher C. Reversal of cocaine-evoked synaptic potentiation resets drug-induced adaptive behaviour. *Nature* 2012;481:71-5.
71. Kim CY, Ku MJ, Qazi R, Nam HJ, Park JW, Nam KS, et al. Soft subdermal implant capable of wireless battery charging and programmable controls for applications in optogenetics. *Nat Commun* 2021;12:535.
72. Qazi R, Gomez AM, Castro DC, Zou Z, Sim JY, Xiong Y, et al. Wireless optofluidic brain probes for chronic neuropharmacology and photostimulation. *Nat Biomed Eng* 2019;3:655-69.
73. Pellegrino LJ, Pellegrino AS, Cushman AJ. *A Stereotaxic Atlas of the Rat Brain*: Plenum Press, New York; 1979.
74. Vanderschuren LJ, Kalivas PW. Alterations in dopaminergic and glutamatergic transmission in the induction and expression of behavioral sensitization: a critical review of preclinical studies. *Psychopharmacology (Berl)* 2000;151:99-120.
75. Yoon HS, Kim S, Park HK, Kim JH. Microinjection of CART peptide 55-102 into the nucleus accumbens blocks both the expression of behavioral sensitization and ERK phosphorylation by cocaine. *Neuropharmacology* 2007;53:344-51.
76. Zaqout S, Kaindl AM. Golgi-Cox Staining Step by Step. *Front Neuroanat*

- 2016;10:38.
77. Sivaguru M, Khaw YM, Inoue M. A Confocal Reflection Super-Resolution Technique to Image Golgi-Cox Stained Neurons. *J Microsc* 2019;275:115-30.
  78. Rodriguez A, Ehlenberger DB, Dickstein DL, Hof PR, Wearne SL. Automated three-dimensional detection and shape classification of dendritic spines from fluorescence microscopy images. *PLoS One* 2008;3:e1997.
  79. Zhang J, Zhang L, Jiao H, Zhang Q, Zhang D, Lou D, et al. c-Fos facilitates the acquisition and extinction of cocaine-induced persistent changes. *J Neurosci* 2006;26:13287-96.
  80. Gorelova N, Yang CR. The course of neural projection from the prefrontal cortex to the nucleus accumbens in the rat. *Neuroscience* 1997;76:689-706.
  81. Rivalan M, Valton V, Seriès P, Marchand AR, Dellsu-Hagedorn F. Elucidating poor decision-making in a rat gambling task. *PLoS One* 2013;8:e82052.
  82. Lee J, Parker KE, Kawakami C, Kim JR, Qazi R, Yea J, et al. Rapidly-customizable, scalable 3D-printed wireless optogenetic probes for versatile applications in neuroscience. *Adv Funct Mater* 2020;30.
  83. Nestler EJ. Molecular basis of long-term plasticity underlying addiction. *Nat Rev Neurosci* 2001;2:119-28.
  84. Robinson TE, Kolb B. Persistent structural modifications in nucleus accumbens and prefrontal cortex neurons produced by previous experience with amphetamine. *J Neurosci* 1997;17:8491-7.
  85. Bourne J, Harris KM. Do thin spines learn to be mushroom spines that remember? *Curr Opin Neurobiol* 2007;17:381-6.
  86. Smith AD, Bolam JP. The neural network of the basal ganglia as revealed by the study of synaptic connections of identified neurones. *Trends Neurosci* 1990;13:259-65.
  87. Cohen S, Greenberg ME. Communication between the synapse and the nucleus in neuronal development, plasticity, and disease. *Annu Rev Cell Dev Biol* 2008;24:183-209.

88. Morgan JI, Curran T. Calcium as a modulator of the immediate-early gene cascade in neurons. *Cell Calcium* 1988;9:303-11.
89. Dos Santos M, Sallery M, Forget B, Garcia Perez MA, Betuing S, Boudier T, et al. Rapid Synaptogenesis in the Nucleus Accumbens Is Induced by a Single Cocaine Administration and Stabilized by Mitogen-Activated Protein Kinase Interacting Kinase-1 Activity. *Biol Psychiatry* 2017;82:806-18.
90. Wiegert JS, Oertner TG. Long-term depression triggers the selective elimination of weakly integrated synapses. *Proc Natl Acad Sci USA* 2013;110:E4510-9.
91. Hasegawa S, Sakuragi S, Tominaga-Yoshino K, Ogura A. Dendritic spine dynamics leading to spine elimination after repeated inductions of LTD. *Sci Rep* 2015;5:7707.
92. Creed M, Pascoli VJ, Lüscher C. Addiction therapy. Refining deep brain stimulation to emulate optogenetic treatment of synaptic pathology. *Science (1979)* 2015;347:659-64.
93. Cardinal RN, Pennicott DR, Sugathapala CL, Robbins TW, Everitt BJ. Impulsive choice induced in rats by lesions of the nucleus accumbens core. *Science (1979)* 2001;292:2499-501.
94. Kwak MJ, Kim WY, Jung SH, Chung YJ, Kim JH. Differential transcriptome profile underlying risky choice in a rat gambling task. *J Behav Addict* 2022;11:845–57.
95. Kim CK, Ye L, Jennings JH, Pichamoorthy N, Tang DD, Yoo AW, et al. Molecular and Circuit-Dynamical Identification of Top-Down Neural Mechanisms for Restraint of Reward Seeking. *Cell* 2017;170:1013-27.e14.
96. Langdon AJ, Hathaway BA, Zorowitz S, Harris CBW, Winstanley CA. Relative insensitivity to time-out punishments induced by win-paired cues in a rat gambling task. *Psychopharmacology (Berl)* 2019;236:2543-56.
97. Vadhan NP, Hart CL, Haney M, van Gorp WG, Foltin RW. Decision-making in long-term cocaine users: Effects of a cash monetary contingency on

- Gambling task performance. *Drug Alcohol Depend* 2009;102:95-101.
98. Wittwer A, Hulka LM, Heinemann HR, Vonmoos M, Quednow BB. Risky Decisions in a Lottery Task Are Associated with an Increase of Cocaine Use. *Front Psychol* 2016;7:640.
99. Ferland JN, Winstanley CA. Risk-preferring rats make worse decisions and show increased incubation of craving after cocaine self-administration. *Addict Biol* 2017;22:991-1001.

## ABSTRACT (IN KOREAN)

코카인 민감화 발현과 도박성게임 동물모델에서 나타나는 위험선택  
의사결정에서 전변연피질-중격측좌핵 중심층 신경회로의 역할

<지도교수 김 정 훈>

연세대학교 대학원 의과학과

구 민 정

약물 및 행위 중독은 갈망 및 의사결정 장애와 같은 임상적 특징을 공유하고, 높은 동반이환을 나타낸다. 이러한 특징은 공통된 신경기질에 의해 나타날 수 있으며, 전두-선조 신경회로는 갈망과 의사결정 장애를 매개하는 주요 신경기질로 연구되어 왔다. 중독 동물모델을 이용한 연구는 유전적 또는 뉴런활성의 조절을 가능하게 함으로써 특정 신경회로의 역할을 보다 정밀하게 연구할 수 있게 한다. 행동 민감화는 약물중독 동물모델로써 약물 갈망의 기저에 있는 신경생물학적 요인을 연구하기 위해 널리 사용되어 왔으며, 코카인 및 암페타민과 같은 정신운동 자극제에 의해 강력하게 유도된다. 쥐를 이용한 도박성 게임 과제(rGT)는 도박중독 동물모델로써 동물의 충동적 의사

결정 및 그와 관련된 신경 메커니즘에 대한 연구를 위해 사용된다. 전변연피질(PL)과 중격측좌핵 중심층(NAc core)을 포함한 일부 뇌 영역이 코카인 갈망과 충동적 의사결정에 모두 관련되어 있다고 보고되었지만, PL-NAc core 신경회로의 역할은 아직 명확하게 밝혀지지 않았다. 따라서 본 연구에서는 PL-NAc core 신경회로가 코카인으로 유도된 행동 민감화 조절 및 rGT에서의 충동적 의사 결정 조절에 관여하는지 연구하였다. 특정 신경회로를 선택적으로 조절하고 동물의 행동 제한을 최소화하기 위해 무선 광유전학 기술을 사용하였다. 코카인 민감화 실험에서 PL-NAc core 신경회로의 광유전학적 자극은 코카인으로 유도된 보행성 민감화를 유의미하게 억제하였다. 또한 NAc core 에서 코카인에 의한 c-Fos 발현 및 버섯모양 수상돌기가시의 밀도 증가를 억제하였다. 이러한 결과는 PL-NAc core 활성화 변화가 버섯모양 수상돌기가시 밀도의 변화를 통하여 코카인 갈망을 약화시킬 수 있음을 나타낸다. rGT 실험에서는 의사결정 직전 PL-NAc core 의 광유전학적 자극이 위험 선호도에 따라 충동적 선택에 차등적으로 영향을 주었다. '위험회피형' 쥐는 광유전학적 자극으로 충동적인 선택이 증가하였으며, 이는 P2 선택 감소 및 P3 선택 증가로 인한 것이었다. 이와 달리, '위험추구형' 쥐는 동일한 광유전학적 자극에도 선택 선호도를 바꾸지 않았다. 하지만 보상먹이를 먹으러 가는 시간이 길어졌고, 보상이 주어지는 트레이에 머리를 넣는 행동 또한 많아졌다. 이러한 결과는 의사결정 직전에 PL-NAc core 활성화가 위험 선호도에 따라 다를 수 있으며, 신경회로의 활성화가 다름에 따라 충동적 의사결

정 또는 도박성 행동에 대한 동기부여에 차등적으로 기여할 수 있음을 의미한다. 종합하면, 본 연구의 결과는 PL-NAc core 신경회로가 코카인 갈망의 조절에 기여할 수 있고, 위험 선호도에 따라 충동적 의사결정 또는 도박에 대한 동기를 차등적으로 매개할 수 있음을 시사한다.

---

핵심되는 말 : 전변연피질, 중격측좌핵 중심층, 코카인 민감화, 도박  
성게임 동물모델, 무선 광유전학

## PUBLICATION LIST

1. Kim CY\*, **Ku MJ**\*, Qazi R, Nam HJ, Park JW, Nam KS, Oh S, Kang I, Jang JH, Kim WY, Kim JH, Jeong JW. Soft subdermal implant capable of wireless battery charging and programmable controls for applications in optogenetics. *Nat Commun.* 2021;12:535.
2. Yoon HS, **Ku MJ**, Cai WT, Kim JH. A novel synthetic cathinone,  $\alpha$ -pyrrolidinopentiothiophenone (PVT), produces locomotor sensitization in rat: Implications for GSK3 $\beta$  connections in the nucleus accumbens core. *Neurochem Int.* 2019;124:25-30.

\* These authors have contributed equally.